0026-895X/04/6606-1465–1477$20.00
MOLECULAR PHARMACOLOGY
Copyright © 2004 The American Society for Pharmacology and Experimental Therapeutics
Mol Pharmacol 66:1465–1477, 2004

Vol. 66, No. 6
5199/1186297
Printed in U.S.A.

Induction of Cyclooxygenase-2 Overexpression in Human Gastric Epithelial Cells by *Helicobacter pylori* Involves TLR2/TLR9 and c-Src-Dependent Nuclear Factor-κB Activation

Ya Jen Chang, Ming Shiang Wu, Jaw Town Lin, Bor Shyang Sheu, Tatsushi Muta, Hiroyasu Inoue, and Ching-Chow Chen

Department of Pharmacology (Y.J.C., C.C.C) and Division of Gastroenterology, Department of Internal Medicine (M.S.W., J.T.L.), College of Medicine, National Taiwan University, and National Taiwan University Hospital, Taipei, Taiwan; Department of Internal Medicine, College of Medicine, National Cheng Kung University, Tainan, Taiwan (B.S.S.); Department of Molecular and Cellular Biochemistry, Graduate School of Medical Sciences, Kyushu University, Fukuoka, Japan (T.M.); and Department of Pharmacology, National Cardiovascular Center Research Institute, Osaka, Japan (H.I.).

Received July 21, 2004; accepted September 20, 2004

ABSTRACT

Gastric epithelial cells were incubated with a panel of clinical isolates of *Helicobacter pylori*, including nonulcer dyspepsia with gastritis (HS, $n = 20$), gastric ulcer (HU, $n = 20$), duodenal ulcer (HD, $n = 21$), and gastric cancer (HC, $n = 20$). HC strains induced a higher cyclooxygenase-2 (COX-2) expression than those from HS, HD, and HU. The bacterial virulence factors and the host cellular pathways were investigated. Virulence genes of *iceA, vacA, babA2, cagA 3′* repeat region, and *hrgA* failed to show any association with the disease status and COX-2 expression. Methylation-specific polymerase chain reaction revealed HC strains not affecting the methylation status of COX-2 promoter. Nuclear factor (NF)-κB, NF-interleukin 6, and cAMP response element were found to be involved in COX-2 induction. We explored a novel NF-κB activation pathway. The mutants of TLR2 and TLR9, but not TLR4, inhibited *H. pylori*-induced COX-2 promoter activity, and neutralizing antibodies for TLR2 and TLR9 abolished *H. pylori*-induced COX-2 expression. Phosphatidylinositol-specific phospholipase C (PI-PLC), protein kinase C (PKC), and Src inhibitors inhibited COX-2 induction. The dominant-negative mutants of NIK and various IκB kinase complexes, including IKKβ (Y188F), IKKβ (Y199F), and IKKβ (FF), inhibited the COX-2 promoter activity. Phosphorylation of GST-IKKβ (132–206) at Tyr^{188} and Tyr^{199} by c-Src was found after *H. pylori* infection. In summary, *H. pylori* induces COX-2 expression via activations of NF-κB, NF-interleukin 6, the cAMP response element. In NF-κB activation, *H. pylori* acts through TLR2/TLR9 to activate both the cascade of PI-PLCγ/PKCα/c-Src/IKKα/β and the cascade of NIK/IKKα/β, resulting in the IκBα degradation and the expression of COX-2 gene. The COX-2 overexpression may contribute to the carcinogenesis in patients colonized with these strains.

Helicobacter pylori has been identified as a major pathogen leading to the development of a wide range of gastroduodenal diseases (Passaro et al., 2002). However, only a small portion of infected patients suffered from the more severe gastric pathological conditions, such as gastric malignancy (Peek and Blaser, 2002). Evidence has emerged that the inappropriate inflammation of gastric mucosa would dictate the clinical outcomes after exposure to *H. pylori* (Bodger and Crabtree, 1998). Clinical outcomes associated with *H. pylori* infection include gastritis, duodenal ulcer, gastric ulcer, gas-

This study was supported by grants from National Health Research Institute (NHRI-EX93-9307BI) and National Science Council (NSC91–2314-B002-390, 91-2315-B002-005), Taiwan.

Y.J.C. and M.S.W. contributed equally to this work.

Article, publication date, and citation information can be found at http://molpharm.aspetjournals.org.
doi:10.1124/mol.104.005199.

ABBREVIATIONS: GC, gastric cancer; COX, cyclooxygenase; NF, nuclear factor; IL, interleukin; CRE, cAMP response element; TLR, Toll-like receptor; LPS, lipopolysaccharide; ICAM, intercellular adhesion molecule; FCS, fetal calf serum; U73122, 1-[6-[[17β-methoxyestra-1,3,5(10)-trien-17-yl]amino]hexyl]-1*H*-pyrrole-2,5-dione; U73343, 1-[6-[[17β-3-methoxyestra-1,3,5(10)-trien-17-yl]amino]hexyl]-2,5- pyrrolidine-dione; Ro 31-8220, 3-[1-[3-(amidinothio)propyl-1H-indol-3-yl]-3-(1-methyl-1H-indol-3-yl)maleimide (Bisindolylmaleimide IX), methanesulfonate; HC, *H. pylori* isolate from gastric cancer; HU, *H. pylori* isolate from gastric ulcer; HD, *H. pylori* isolate from duodenal ulcer; HS, *H. pylori* isolate from gastritis; PBS, phosphate-buffered saline; m.o.i., multiplicity of infection; Ab, antibody; PCR, polymerase chain reaction; EMSA, electrophoretic mobility shift assay; wt, wild type; PI-PLC phosphoinositide-specific phospholipase C; PKC, protein kinase C; TNF, tumor necrosis factor; C/EBP, CCAAT/enhancer-binding protein; CREB, cAMP response element-binding protein; KBM, κB site mutation; ILM, NF-IL6 site mutation; CRM, CRE site mutation; P/H, proline→histidine; ICD, Intracellular domain deletion; PP2, 4-amino-5-(4-chlorophenyl)-7-(*t*-butyl)pyrazolo[3,4-*d*]pyrimidine; K/R, lysine→arginine; SH2(N), arginine564→alanine; GST, glutathione *S*-transferase; bp, base pair(s).

tric adenocarcinoma, and gastric mucosa-associated lymphoid tissue lymphoma (Parsonnet et al., 1991). Both host factors and the characteristics of infecting strains have been postulated to contribute to the variable outcome and have been the focus of intensive investigations (Blaser, 2002). The reported strain-specific virulence factors for gastric cancer (GC) include CagA, VacA, IceA, BabA2, and HrgA (Yamaoka et al., 1998; Kidd et al., 2001; Nogueira et al., 2001; Prinz et al., 2001; Ando et al., 2002; Bravo et al., 2002).

Cyclooxygenase (COX)-2 is the key enzyme responsible for the prostaglandin production during gastric inflammation and ulcer healing (Jackson et al., 2000). The overexpression of COX-2 has been implicated in the development and progression of GC (van Rees et al., 2002). *H. pylori* infection is the most important factor for the induction of COX-2 in the stomach. Both animal studies and human samples have confirmed that *H. pylori*-induced inflammation is linked to COX-2 expression (Takahashi et al., 2000). The degree of COX-2 expression is strongly correlated with the extent of inflammation and the severity of gastric disease (Sung et al., 2000). In addition, levels of the COX-2 protein were significantly higher in patients suffering from gastric cancer who were infected with *H. pylori* than in those with nonulcer dyspepsia (Wambura et al., 2002), and the up-regulation of COX-2 in *H. pylori*-associated GC is related to vascular invasion (Chen et al., 2001). Therefore, COX-2 expression was assumed to play a crucial role in *H. pylori*-associated GC in addition to gastric inflammation. Recent in vitro studies demonstrated the modulation of COX-2 expression by *H. pylori* (Romano et al., 1998). It is of interest to investigate whether *H. pylori* isolates from patients with different disease status vary in their capabilities to induce COX-2 expression, because such data are limited. Furthermore, the roles of *hrgA, iceA, vacA, babA2*, and *cagA* genotypes in relation to COX-2 expression and disease status are also determined.

The induction of COX-2 expression requires the de novo mRNA and protein synthesis (Kosaka et al., 1994), indicating the regulation at transcriptional level. The promoter region of human COX-2 gene has been cloned and sequenced and has been shown to contain the putative recognition sequences for several transcriptional factors, including two NF-κB sites, a nuclear factor for IL-6 expression (NF-IL6)/C/EBP, an activator protein 1, and a cAMP response element (CRE) (Kosaka et al., 1994). Although NF-κB activation by *H. pylori* has been reported previously (Keates et al., 1997), whether it is involved in the *H. pylori*-induced COX-2 expression and whether other transcriptional factor is also activated was not explored. These issues are addressed in the present study.

It has been reported that epithelial cells and macrophages recognize microbial infections via Toll-like receptors (TLRs) (Rock et al., 1998). These receptors are oligospecific and recognize conserved motifs on pathogens. So far, 10 human TLRs have been identified (Rock et al., 1998), and their ligands are beginning to be unraveled. TLR4 recognizes lipopolysaccharide (LPS), which is the major outer membrane component of Gram-negative bacteria (Poltorak et al., 1998). TLR2 is involved in the recognition of Gram-positive bacteria (Takeuchi et al., 1999). TLR9 recognizes bacterial DNA (Hemmi et al., 2000). In this study, the types of TLRs and their role in *H. pylori*-regulated COX-2 expression are evaluated.

The phosphorylations of Ser^{177} and Ser^{181} on IKKβ by the upstream mitogen-activated protein kinase kinase kinase leading to NF-κB activation are well recognized (Malinin et al., 1997). However, our recent studies found the additional phosphorylations of Tyr^{188} and Tyr^{199} by c-Src through PKC activation resulting in COX-2 and ICAM-1 expressions (Huang et al., 2003a,b). The upstream signaling molecule involving in *H. pylori*-induced NF-κB activation is investigated in the present study. Whether the PKC/c-Src/IKKβ pathway is also involved in the *H. pylori*-induced NF-κB activation leading to COX-2 expression is examined to determine whether this pathway exists in different types of cells despite different stimuli.

Materials and Methods

Materials. The rabbit polyclonal antibodies specific to TLR2, TLR4, IκBα, IKKβ, and c-Src and the goat polyclonal antibodies specific to COX-2, COX-1, TLR9, and actin were purchased from Santa Cruz Biotechnology (Santa Cruz, CA). Human recombinant TNF-α was purchased from R&D Systems (Minneapolis, MN). RPMI, fetal calf serum (FCS), penicillin, and streptomycin were obtained from Invitrogen (Carlsbad, CA). Staurosporine was obtained from Sigma (St. Louis, MO). U73122, U73343, and PP2 were obtained from Calbiochem (San Diego, CA). Reagents for SDS-polyacrylamide gel electrophoresis were from Bio-Rad (Hercules, CA). T4 polynucleotide kinase was from New England Biolabs (Beverly, MA), poly(dI-dC) was from Amersham Biosciences, [γ-^{32}P]ATP (3000 Ci/mmol) was from PerkinElmer Life and Analytical Sciences (Boston, MA), the SuperFect reagent was from QIAGEN (Valencia, CA), and the luciferase assay kit was from Promega (Madison, WI).

Bacterial Strains and Growth Conditions. We studied *H. pylori* strains from patients undergoing gastroscopy for the evaluation of upper gastrointestinal symptoms. At the time of gastroscopy, two biopsy specimens were taken from antrum for bacterial culture. A total of 81 clinical isolates from patients with nonulcer dyspepsia with gastritis (HS, $n = 20$), gastric ulcer (HU, $n = 20$), duodenal ulcer (HD, $n = 21$), and gastric cancer (HC; $n = 20$, 11 from intestinal type and nine from diffuse type) were collected. Columbia agar with 5% sheep blood (Invitrogen) was used for *H. pylori* culture. The bacterial cells were cultured at 37°C in a microaerophilic chamber (Don Whitley, West Yorkshire, England) containing 10% CO_2, 5% O_2, and 85% N_2. Bacterial cells were grown to 48 h on Columbia agar plates, collected, washed with PBS, pH 7.4, and pelleted. Cell pellets were then resuspended in PBS, pH 7.4, and used for infection experiment (Wang et al., 1998).

Cell Culture and *H. pylori* Infection Experiments. The human gastric cancer epithelial cell lines AGS and MKN45 were obtained from the American Type Culture Collection (Manassas, VA) and RIKEN (Saitama, Japan), respectively. Both were cultured in RPMI 1640 supplemented with 10% FCS, 100 U/ml of penicillin, and 100 μg/ml of streptomycin. AGS cells and *H. pylori* were cocultured in antibiotic-free RPMI 1640 supplemented with 10% FCS. Bacteria were resuspended in PBS, pH 7.4, and diluted corresponding to the multiplicity of infection (m.o.i.) at 150:1. Cells were incubated in the absence (controls) or in the presence of bacteria for 16 h.

Preparation of Cell Extracts and Western Blot Analysis. After 16 h incubation with *H. pylori*, AGS or MKN45 cells were rapidly washed with PBS to remove bacteria and then lysed with the ice-cold lysis buffer (50 mM Tris-HCl, pH 7.4, 1 mM EGTA, 1 mM NaF, 150 mM NaCl, 1 mM phenylmethylsulfonyl fluoride, 5 μg/ml leupeptin, 20 μg/ml aprotinin, 1 mM Na_3VO_4, 10 mM β-glycerophosphate, 5 mM sodium pyrophosphate, and 1% Triton X-100). The cell lysate was subjected to SDS-polyacrylamide gel electrophoresis using 10% running gels. The proteins were transferred to the nitrocellulose paper, and the Western blot was performed as described

previously (Huang et al., 2003b). The quantitative data were obtained using a computing densitometer with ImageQuant software and normalized by the actin expression (Amersham Biosciences).

Immunofluorescence Staining. AGS or MKN45 cells grown on coverslips were cocultured for 16 h with *H. pylori* in antibiotic-free growth medium, rapidly washed with PBS, then fixed at room temperature for 30 min with 3.7% paraformaldehyde. After washing with PBS, the cells were blocked for 30 min with 3% bovine serum albumin in Tris-buffered saline-Tween 20 containing 0.1% Triton X-100, then incubated with anti-COX-2 Ab (1:100) for 1 h, washed extensively, and stained for 30 min with anti-goat IgG-fluorescein (1:2000). After further washes, the coverslips were mounted on glass slides using mounting medium (2% *n*-propyl gallate in 60% glycerol and 0.1 M PBS, pH 8). Optical sections of the immunostained cells were observed and photographed using a Zeiss Axiovert inverted microscope equipped with a photoMicroGraph Digitized Integration System (Zeiss, Oberkochen, Germany).

RT-PCR. Total RNA was isolated from AGS cells using TRIzol reagent (Invitrogen). The reverse transcription reaction was performed using 2 μg of total RNA that was reverse-transcribed into cDNA using the oligo-dT primer, then the cDNA was amplified for 30 cycles using two oligonucleotide primers derived from a published COX-2 sequence (5′-CAGCACTTCACGCATCAGTT-3′ and 5′-TCTGGTCAATGGAAGCCTGT-3′) and two oligonucleotide primers from a β-actin sequence (5′-TGAC GGGGTCACCCACACTGTGCCCATCTA-3′ and 5′-CTAGAAGCATTTGCGGGGACGATGGAGGG-3′). For COX-2, a polymerase chain reaction (PCR) cycle consisted of a denaturation step (94°C, 1 min), an annealing step (60°C, 1 min), and an elongation step (72°C, 1.5 min). There were 35 cycles, followed by an additional extension step (72°C, 7 min). For β-actin, PCR cycle was carried out for 30 s at 94°C, 30 s at 65°C, and 1 min at 70°C. The PCR products were subjected to electrophoresis on a 1.5% agarose gel. Quantitative data were obtained using a computing densitometer and ImageQuant software (Amersham Biosciences).

Detection of iceA, cagA 3′ Repeat Region, hrgA, babA2, and vacA Genotypes. PCR with specific primers was used to detect genotypes of *H. pylori* as described previously (Yamaoka et al., 1998; Kidd et al., 2001; Ando et al., 2002; Wang et al., 1998; Sheu et al., 2003). The primers used are shown in Table 1. The amplification condition was denatured at 94°C for 5 min, followed by 35 cycles of 94°C for 1 min, 50°C for 1 min, and 72°C for 1 min, and a final extension at 72°C for 5 min (for *cagA, hrgA*, and *iceA*). The annealing temperature was changed to 55°C for *vacA* and 45°C for *babA2*. All samples with negative results were tested at least twice. The strains from randomly selected samples with positive PCR results were subjected for sequencing using an ABI Prism 377 DNA sequencer (Applied Biosystems, Foster City, CA).

TABLE 1
Primers

ice A (Kidd et al., 2001)	
Forward	5′-GTTGGGTATATCACAATTAT-3′
Reverse	5′-TTACCCTATTTTCTAGTAGGT-3′
CagA (Yamaoka et al., 1998)	
Forward	5′-ACCCTAGTCGGTAATGGGTTA-3′
Reverse	5′-GTAATTGTCTAGTTTCGC-3′
hrgA	
Forward	5′-TCTCGTGAAAGAGAATTTCC-3′
Reverse	5′-TAAGTGTGGGTATATCAATC-3′
hpyIIIR (Ando et al., 2002)	
Forward	5′-CTCATTGCTGTGAGGGAT-3′
Reverse	5′-TCTTGATAGGATCTTGCG-3′
babA2 (Sheu et al., 2003)	
Forward	5′-CCAAACGAAACAAAAAGCGT-3′
Reverse	5′-GCTTGTGTAAAAGCCGTCGT-3′
vacA s1a	
Forward	5′-GTCAGCATCACACCGCAAC-3′
Reverse	5′-CTGCTTGAATGCGCCAAACTTTATC-3′
vacA s2	
Forward	5′-GCTAACACGCCAAATGATCC-3′
Reverse	5′-CTGCTTGAATGCGCCAAACTTTATC-3′
vacA m1	
Forward	5′-GGCCACAATGCAGTCATGG-3′
Reverse	5′-CTCTTAGTGCCTAAAGAAACA-3′
vacA m2 (Wang et al., 1998)	
Forward	5′-GGAGCCCCAGGAAACATTG-3′
Reverse	5′-CATAACTAGCGCCTTGCAC-3′

Methylation Status of the COX-2 Promoter. The methylation status of the COX-2 promoter was determined by methylation-specific PCR as detailed previously (Akhtar et al., 2001). In brief, 1 μg of genomic DNA isolated from AGS cells was bisulfite-modified. PCR was performed with unmethylated primers [5′-ATAGATTATATGGTGGTGGTGGT-3′/5′-CACAATCTTTACCCAAACACTTCC-3′ (171-bp product)] and methylated primers [5′-TTAGATACGGCGGCGGCGGC- 3′/5′-TCTTTACCCGAACGCTTCCG3′ (161-bp product)]. The PCR condition was 30 s at 95°C, 45 s at 65°C, 45 s at 72°C for 35 cycles followed by a final 5-min extension at 72°C.

Preparation of Nuclear Extracts and the Electrophoretic Mobility Shift Assay. AGS cells were cocultured with *H. pylori* isolates from patients with GC for 30, 60, or 120 min, and then nuclear extracts were prepared as described previously (Huang et al., 2003a). Oligonucleotides corresponding to the downstream κB (5′-GAGTG**GGGACTACCC**CCTC-3′), NF-IL6 (5′-CGGC**TTACGCAAT**TTTT-3′), and CRE (5′-TCA**TTTCGTCA**CATG-3′) consensus sequences in the human COX-2 promoter were synthesized, annealed, and end-labeled with [γ-^{32}P]ATP using T4 polynucleotide kinase, and EMSA was performed as described previously (Huang et al., 2003b). Bold letters represent the binding sequences for transcription factor.

Plasmids. The COX-2 promoter constructs pGS-459/+9, −327/+59, CRM, ILM, or KBM (Luc) were generous gifts from Dr. L. H. Wang (University of Texas, Houston, TX). NF-κB luciferase reporter (κB-Luc) was from Stratagene (La Jolla, CA). The PLC-γ2 wild type and the mutant SH2(N), in which the Arg at position 564 is replaced by Ala, and the PKC-α constitutively active mutant (PKC-α AE) and the PKC-α dominant-negative mutant (PKCα/KR) were gifts from Drs. T. Kurosaki (Kansai Medical University, Japan) and A. Altman (La Jolla Institute for Allergy and Immunology, San Diego, CA) respectively. The dominant-negative mutants of NIK (KKAA), IKKα (KM), and IKKβ (KM) were gifts from Signal Pharmaceuticals (San Diego, CA). The dominant-negative mutant of IKKβ (AA) was from Dr. Karin (University of California San Diego, San Diego, CA). pGEX-IκB$\alpha\alpha$ (1–100) was a gift from Dr. Nakano (University of Juntendo, Tokyo, Japan). pGEX-IKKβ (132–206) was a gift from Dr. Nakanishi (University of Nagoya, Nagoya, Japan). TLR2 and TLR4 plasmids, including wt TLR2, wt TLR4, mutants of TLR2 (P/H) and TLR4 (P/H) were as described previously (Muta and Takeshige, 2001). TLR9 plasmids including wt TLR9 and mutant of TLR9 (ICD) from Ken J. Ishii (United States Food and Drug Administration, Bethesda, MD) were as described previously (Takeshita et al., 2001). The dominant-negative mutants of c-Src (K295M), IKKβ (Y188F), IKKβ (Y199F), and IKKβ (YYFF) were prepared as described previously (Huang et al., 2003b).

Transient Transfection and Luciferase Activity Assay. AGS cells grown to 60% confluence in 12-well plates were transfected with either the human COX-2 promoter construct or kB-Luc using SuperFect (Qiagen) according to the manufacturer's recommendations. In brief, reporter DNA (0.3 μg) and β-galactosidase DNA (0.15 μg; pRK plasmid containing the β-galactosidase gene driven by the constitutively active simian virus 40 promoter was used to normalize the transfection efficiency) were mixed with 0.45 μl of SuperFect in 0.4 ml of serum-free RPMI 1640. After 10 to 15 min of incubation at room temperature, the mixture was applied to the cells. Six hours later, 0.4 ml of RPMI 1640 with 20% FCS was added. Twenty-four hours after transfection and change to an antibiotic-free medium, the cells were incubated with *H. pylori* isolate from GC patients for 6 h. Cell extracts were then prepared, and the luciferase and β-galactosidase activities were measured. The luciferase activity was normalized to

the β-galactosidase activity. In experiments using dominant-negative mutants, cells were cotransfected with reporter (0.3 μg) and β-galactosidase (0.15 μg) and either the dominant-negative TLRs, PLCγ2, PKCα, NIK, IKKα, IKKβ, and c-Src mutants or the empty vector (0.6 μg). In experiments using wt plasmids, cells were cotransfected with 0.3 μg of reporter plasmid, 0.15 μg of β-galactosidase plasmid, 0.45 μg of the wt PLCγ2, constitutively active PKCα (A/E) plasmid, wt c-Src plasmid, or empty vector, and 0.6 μg of the dominant-negative PLCγ2, PKCα, NIK, IKKα, IKKβ, or c-Src mutant or empty vector.

Immunoprecipitation and Kinase Activity Assay. After incubation with *H. pylori* isolates from patients with GC, with or without 30-min pretreatments with PI-PLC, PKC, and Src kinase inhibitors, AGS cells were rapidly washed with PBS and lysed with ice-cold lysis buffer (50 mM Tris-HCl, pH 7.4, 1 mM EGTA, 150 mM NaCl, 1% Triton X-100, 1 mM phenylmethylsulfonyl fluoride, 5 μg/ml of leupeptin, 20 μg/ml of aprotinin, 1 mM NaF, and 1 mM Na_3VO_4), then either IKK or c-Src was immunoprecipitated. For the in vitro kinase assay, 100 μg of total cell extract was incubated for 1 h at 4°C with either 0.5 μg of rabbit anti-IKKβ or anti-c-Src Ab. The protein A-Sepharose CL-4B beads were then added to the mixture, and incubation continued for 4 h at 4°C. The immunoprecipitates were collected by centrifugation, washed three times with lysis buffer without Triton X-100, and then incubated for 30 min at 30°C in 20 μl of kinase reaction mixture (20 mM HEPES, pH 7.4, 5 mM $MgCl_2$, 5 mM $MnCl_2$, 0.1 mM Na_3VO_4, and 1 mM dithiothreitol) containing 10 μM [γ-^{32}P]ATP and either 1 μg of bacterially expressed GST-IκBα (1–100) as IKK substrate, 1 μg of acidic denatured enolase, or 6 μg of bacterially expressed GST-IKKβ (132–206) as c-Src substrate. The reaction was stopped by the addition of an equal volume of Laemmli buffer, the proteins were separated by electrophoresis on 10% SDS polyacrylamide gels, and the phosphorylated-GST-IκBα (1–100), phosphorylated enolase, and phosphorylated GST-IKKβ (132–206) were visualized by autoradiography. Quantitative data were obtained using a densitometer with ImageQuant software and normalized by the protein expression.

Statistical Analysis. To establish the significance of the results, the Student's *t* test was used for numerical data. Fisher's exact test or χ^2 test was used for categorical data as appropriate. A *p* value less than 0.05 was considered statistically significant.

Results

COX-2 Protein Expression Induced by *H. pylori* Isolates from Patients with Different Disease Status. Compared with basal levels, overexpression of COX-2 protein was seen in the AGS cells treated with either TNF-α or HC at a bacterium/cell ratio of 50:1, 150:1, or 350:1. In contrast, HS and HD showed no obvious COX-2 overexpression [Fig. 1A, (a)]. At a bacterium/cell ratio of 150:1, the capabilities of representative HS, HU, HD, and HC to induce COX-2 expression were shown in Fig. 1A, (b). The clinical isolate from GC had a greater capability to induce COX-2 protein expression, whereas relatively lower induction of COX-2 protein among isolates of nonulcer dyspepsia, gastric ulcer, and duodenal ulcer was seen. To determine whether *H. pylori*-induced COX-2 expression occurred at the transcriptional level, the induction of COX-2 mRNA expression stimulated by HC in AGS cells was examined by RT-PCR and a time-dependent increase was found [Fig. 1A, (c)]. A box plot of COX-2 protein expression in AGS cells induced by different clinical isolates is shown in Fig. 1B. The increase induced by these 20 isolates from gastric cancer (6.19 ± 0.86-fold, mean ± S.E.) was significantly higher than that from nonulcer dyspepsia (1.48 ± 0.16-fold; $p < 0.001$), gastric ulcer (1.92 ± 0.38-fold; $p < 0.001$), and duodenal ulcer (1.97 ± 0.46-fold; $p < 0.001$) (Fig. 1B). Compared with HS, HU, and HD, HC also exhibited a stronger ability to induce the COX-2 expression in MKN45 cells, another gastric adenocarcinoma cell line (Fig. 1C).

The induction of COX-2 by HC in AGS and MKN45 cells was further demonstrated by immunofluorescence staining. As shown in Fig. 1D, no COX-2 expression was seen in the basal state but was apparent in the nuclear envelope of AGS cells and in the cytosol of MKN45 cells after coculture with HC.

Genotypes of *H. pylori* Isolates from Patients with Different Disease Status. Table 2 shows the genotypes of *hrg, iceA, babA2, cagA*, and *vacA* from 20 patients of HS, HU, and HC, and 21 patients of HD. There was no difference in the genotypes among the *H. pylori* isolates from patients with different disease status despite the higher COX-2 induction capability of HC. Furthermore, no difference in COX-2 induction capability was seen among HC isolates from 11 intestinal and nine diffused subtypes of GC. Regardless of the difference in induction capacity, all *H. pylori* strains can induce COX-2 expression in MKN45 cells (Fig. 1C), suggesting that *H. pylori*-induced COX-2 expression is a common phenomenon. To further study the mechanism of this effect, the *H. pylori* isolates that exhibited stronger ability of inducing COX-2 overexpression were chosen for the following studies using AGS cells.

***H. pylori*-Induced COX-2 Promoter Activity via NF-κB, C/EBP, and CREB Activation without Change in the Methylation Status.** To analyze the transcriptional regulation, the methylation status of COX-2 promoter in AGS cells before and after incubation with *H. pylori* was examined. By methylation-specific PCR, both the unmethylated and methylated products were shown before the incubation with *H. pylori* (Fig. 2A, lanes 1–2). The incubation with *H. pylori* did not affect the methylation status (Fig. 2A, lanes 3–4).

To identify which *cis*-acting element was involved, the COX-2 promoter-Luc constructs, including −327/+59, KBM with κB site (−223/−214) mutation, ILM with NF-IL6 site (−132/−124) mutation, and CRM with CRE site (−59/−53) mutation, were used (Huang et al., 2003b). Our results showed a decrease in the induction of COX-2 promoter activity by *H. pylori* using KBM, ILM, and CRM (Fig. 2B), demonstrating that NF-κB, NF-IL6, and CRE elements contribute to the *H. pylori*-induced COX-2 transcription.

Because NF-κB, NF-IL6, and CRE elements were involved in the COX-2 gene transcription after *H. pylori* infection, the DNA-protein complex formation was examined with the use of EMSA. An increase in NF-κB DNA-protein binding was seen after coculture with *H. pylori* for 30 min and reached a maximum at 60 min (Fig. 2C). Similar induction of C/EBP and CREB DNA-protein complex formation was also seen after 60 and 120 min of coculture (Fig. 2C).

Involvement of Toll-Like Receptors in *H. pylori*-Mediated COX-2 Expression. Several studies have shown the involvement of TLRs in bacterial infections (Rock et al.,1998), whether TLR is involved in the *H. pylori*-induced NF-κB activation leading to COX-2 expression is elucidated. Expression levels of TLR2, TLR4, and TLR9 were found in AGS and MKN45 cells (Fig. 3A), and we examined their role in the *H. pylori*-induced COX-2 promoter activity. As shown in Fig. 3B, the induction of COX-2 promoter activity by *H.*

pylori was inhibited in a dose-dependent manner by the mutant of TLR2 (P/H) and TLR9 (ICD), but not TLR4 (P/H), indicating the involvements of TLR2 and TLR9 but not TLR4. The neutralizing antibody for TLR2 and TLR9 also attenuated the *H. pylori*-induced COX-2 expression (Fig. 3C). To further identify the TLRs-mediated COX-2 promoter activity and its downstream signaling, we overexpressed the wild-type TLRs in AGS cells. The wt TLR2, but not the wt TLR4, increased the COX-2 promoter activity (Fig. 3D). Although TLR9 mutant blocked the induction of *H. pylori*-mediated COX-2 promoter activity, the wt TLR9 was unable to induce the COX-2 promoter activity (Fig. 3D). Combination of TLR2 or TLR9 with *H. pylori* by transfected cells with TLR2 or TLR9 followed by *H. pylori* coculture showed a synergistic effect on the COX-2 promoter activity (Fig. 3D), confirming their involvement in *H. pylori*-mediated COX-2 induction. Although HS alone had no effect on COX-2 induction, the increases of COX-2 promoter activity were seen in the presence of overexpression of TLR2 and TLR9 but not TLR4 (Fig. 3D).

Because TLR2 and TLR9 were demonstrated to be involved in *H. pylori*-induced COX-2 promoter activity (Fig. 3E), their role in *H. pylori*-induced NF-κB activity was examined. As shown in Fig. 3E, HC, but not HS, HU, or HD, induced NF-κB activation, and the dominant-negative mutants of TLR2 and TLR9 inhibited this effect.

Involvements of PLCγ, PKC, and c-Src in *H. pylori*-Mediated COX-2 Expression. The COX-2 expression induced by *H. pylori* was inhibited by either 10 μM U73122 (PI-PLC inhibitor) or 1 μM Ro 31-8220 (PKC inhibitor), whereas 10 μM U73343 (an inactive analog of U73122) had no effect (Fig. 4A, lanes 3–5), indicating the involvement of PI-PLC/PKC pathway. The Src inhibitor PP2 also abolished the *H. pylori*-induced COX-2 expression (Fig. 4A, lane 6), suggesting the role of Src kinase in this regulation. To further confirm the involvement of the PI-PLC/PKC pathway in

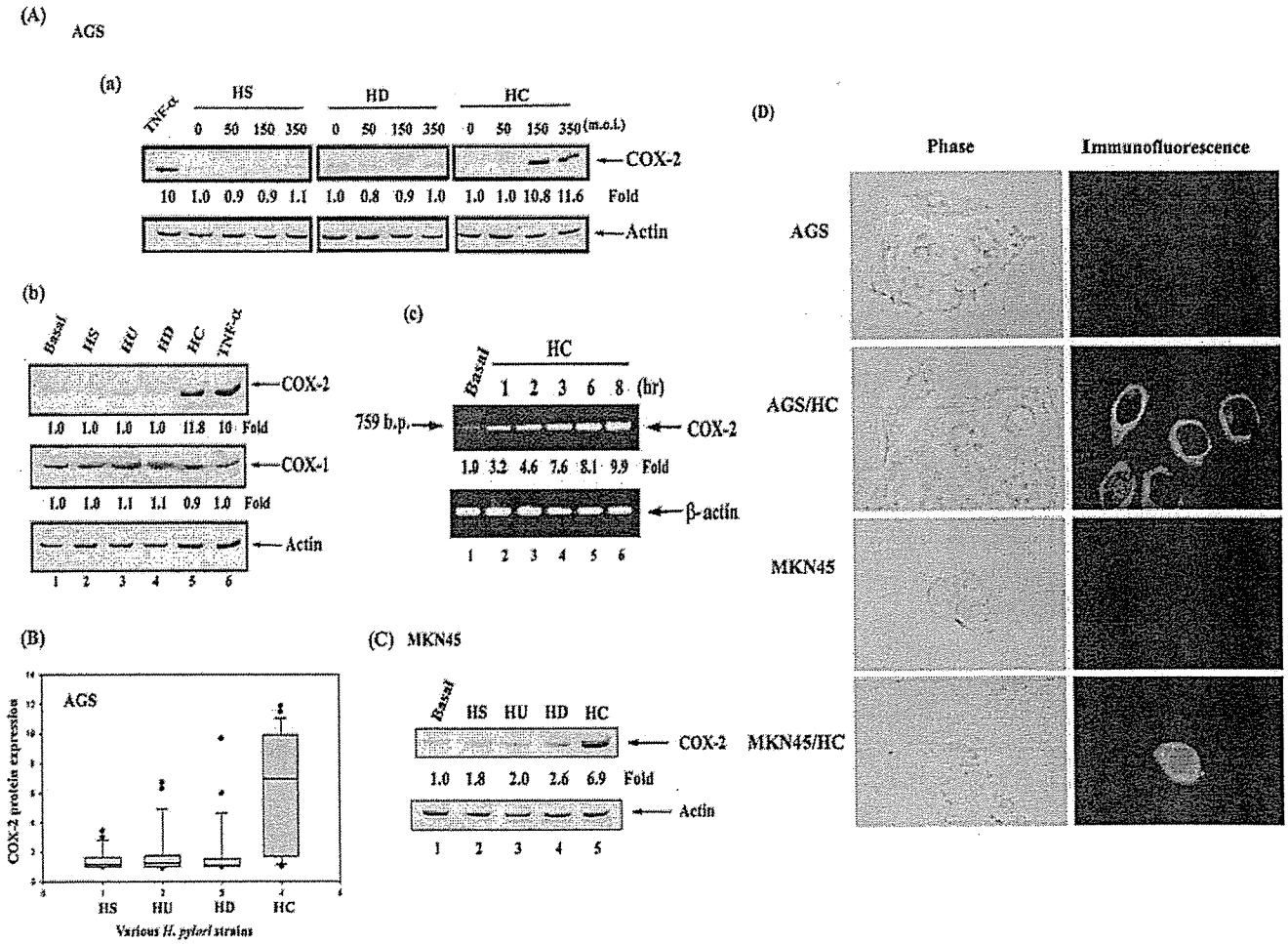

Fig. 1. COX-2 expression in AGS and MKN45 cells induced by *Helicobacter pylori* isolates from patients with gastritis (HS), gastric ulcer (HU), duodenal ulcer (HD), gastric cancer (HC) and by TNF-α. Cells were treated with *H. pylori* isolates from different patients at indicating bacterium/cell ratio in (a) or at a bacterium/cell ratio of 150:1 in (b) and (c) or 10 ng/ml of TNF-α for 16 h. Whole-cell lysates were prepared and subjected to Western blotting using antibody specific for COX-2, COX-1, or Actin. In (c), AGS cells were cocultured with HC for the indicated time. Total RNA (2 μg) was used for RT-PCR as described under *Materials and Methods*. B, box plot of COX-2 expression in AGS cells summarized from different clinical isolates of *H. pylori*. Cells were cocultured with *H. pylori* strains from patients with gastritis (HS) (n = 20), gastric ulcer (HU) (n = 20), duodenal ulcer (HD) (n = 21), and gastric cancer (HC) (n = 20). The quantitative data were normalized by the actin level. In D, COX-2 is located around the nuclear envelope or cytosol. Immunofluorescence staining of AGS or MKN45 cells with affinity-purified anti-COX-2 Ab (1:100) were performed as described under *Materials and Methods*. Control AGS and MKN45 cells or those cocultured with HC for 16 h are shown.

H. pylori-induced COX-2 expression (Fig. 4A), cotransfections of the PLCγ mutant with reporter, the dominant-negative mutants of PKCα (K/R) with reporter, and the c-Src (KM) with reporter were performed. The induction of COX-2 promoter activity by *H. pylori* was attenuated by PLCγ2 (SH2(N)), PKCα (K/R), and c-Src (KM) in a dose-dependent manner, confirming the involvement of these signaling molecules in the COX-2 expression.

TABLE 2
The relationship between the extent of cyclooxygenase-2 expression in AGS cells and genotypes in different clinical isolates of *H. pylori*

	HS (n = 20)	HU (n = 20)	HD (n = 21)	HC (n = 20)
COX-2 expression				
Mean ± S.E.	1.48 ± 0.16	1.92 ± 0.38	1.97 ± 0.46	6.19 ± 0.89*
Restriction endonuclease-replacing gene				
hrgA	7	8	7	7
hpyIIIR	13	12	14	13
IceA				
A1A1	17	18	18	17
A1A2	2	1	2	2
A2A2	1	1	1	1
babA2				
positive	20	20	21	20
negative	0	0	0	0
CagA 3′ repeat region				
A	19	18	21	19
B, C, D	1	2	0	1
vacA				
s1a/m1	3	6	8	6
s1a/m2	17	14	13	14

* $P < 0.001$ versus HS, HU, or HD.

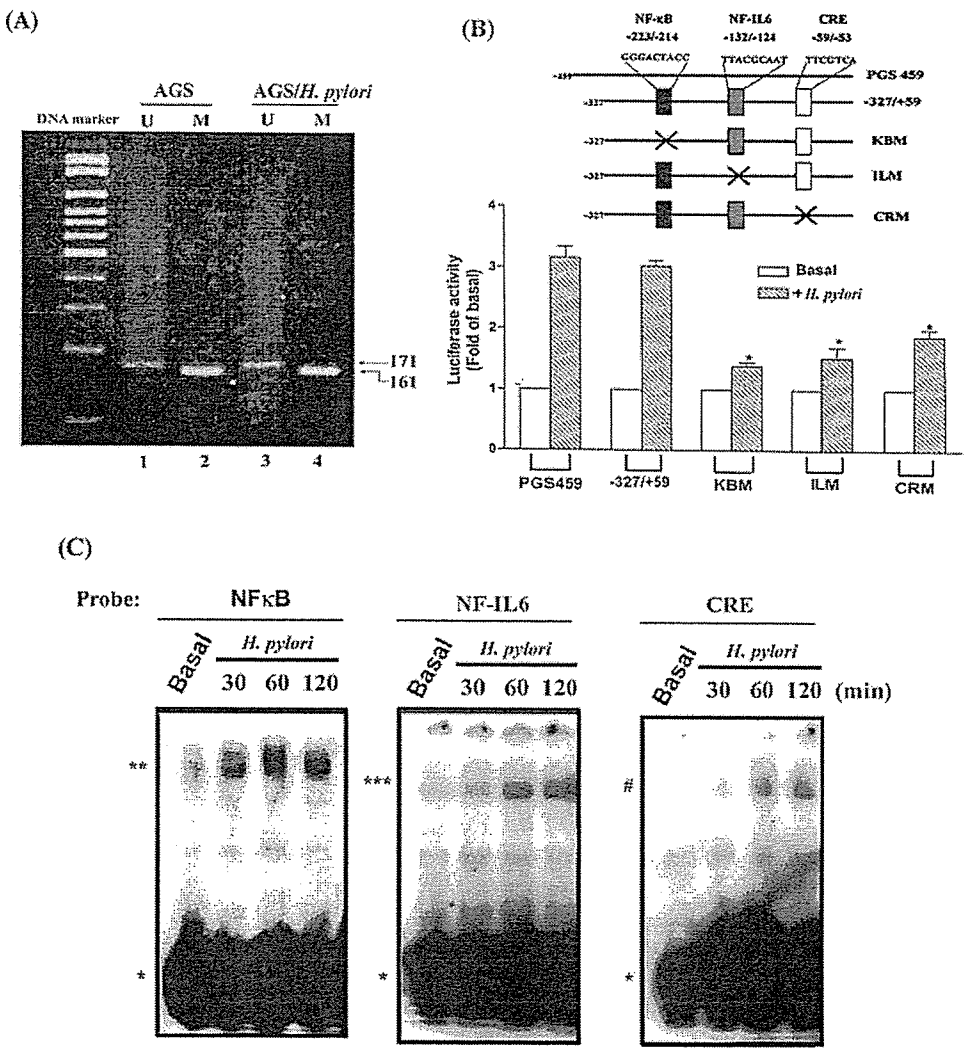

Fig. 2. Methylation status and activation of the COX-2 promoter, and kinetics of DNA-protein complex formation induced by *Helicobacter pylori*. A, methylation-specific PCR was performed after bisulfite modification of DNA as described under *Materials and Methods*. *M* indicates methylated COX-2 and *U* indicates unmethylated COX-2. B, top, schematic diagram of the 5′ regulatory region of the human COX-2 gene. Rectangles indicate the location of the NF-κB, NF-IL6, and CRE sites. Cells were transfected with the pGS459/+9, −327/+59, KBM, ILM, or CRM luciferase expression vector, and then infected with *H. pylori*. Cell extracts were prepared and assayed for luciferase and β-galactosidase activity. The luciferase activity was normalized using the β-galactosidase activity and expressed as the mean ± S.E.M. of three independent experiments performed in triplicate. *, $p < 0.05$ compared with −327/+59. C, cells were cocultured with *H. pylori* (m.o.i., 150) for 30 min, 1 h, or 2 h, then nuclear extracts were prepared. NF-κB, NF-IL6, or CRE oligonucleotide probe was used to measure the DNA-protein complex formation by EMSA as described under *Materials and Methods*. *, free probe; **, NF-κB DNA-protein complex; ***, NF-IL6 DNA-protein complex; #, CRE DNA-protein complex.

Demonstration of TLR2/PLCγ/PKC/c-Src/IKK Pathway in *H. pylori*-Mediated COX-2 Promoter Activity. Involvements of NIK and IKKα/β in the *H. pylori*-induced COX-2 promoter activity were demonstrated using the dominant-negative mutants of NIK (KKAA), IKKα (KM), IKKβ (KM), IKKβ (AA), IKKβ (Y188F), IKKβ (Y199F), and IKKβ (YYFF) [Fig. 5A, (a)]. wt TLR2-induced COX-2 promoter activity was inhibited by either the PLCγ2 mutant or the dominant-negative mutants of PKCα (K/R), c-Src (KM), NIK(KKAA), IKKα (KM) and IKKβ (KM), IKKβ(Y188F), IKKβ(Y199F) and IKKβ(YYFF) [Fig. 5A, (b)], suggesting that *H. pylori* induced COX-2 expression through the activation of PLCγ2, PKCα, c-Src, NIK, IKKα, and IKKβ.

To characterize the relationship between PLCγ2, PKCα, c-Src, and IKKβ, overexpression of the constitutively active PKCα(A/E), wt PLCγ2, and wt c-Src were performed. wt PLCγ2, PKCα (A/E), and wt c-Src increased the COX-2 promoter activity by 7.7-, 2.5-, and 42-fold, respectively (Fig. 5B). The COX-2 promoter activity induced by either wt PLCγ2 or PKCα (A/E) was inhibited by the dominant-negative PKCα (K/R), c-Src (KM), IKKα (KM), and IKKβ (KM) mutants [Fig. 5B, (a) and (b)], whereas that induced by wt c-Src was inhibited by the dominant-negative IKKα (KM) and IKKβ (KM), IKKβ (YF) and IKKβ (YYFF), but not IKKβ (AA) and PLCγ2 (SH2(N)) mutants [Fig. 5B, (c)]. These results indicated the involvement of PI-PLCγ/PKC/c-Src/IKKα/β pathway in *H. pylori*-induced COX-2 expression.

Our recent studies have revealed that phosphorylation of IKKβ at Tyr^{188} and Tyr^{199} is required for the TNF-α-induced ICAM-1 and COX-2 expressions in the lung epithelial cells and also demonstrated that these two tyrosine residues are the targets of c-Src (Huang et al., 2003a,b). Overexpressions of the dominant-negative tyrosine mutants IKKβ (Y188F), IKKβ (Y199F), and IKKβ (YYFF) attenuated the *H. pylori*-induced, the wt TLR2-induced, and the wt c-Src-induced COX-2 promoter activity. The dominant-negative IKKβ (KM) mutant with Lys^{44} mutated to methionine had a similar inhibitory effect (Fig. 5, A and B). On the other hand, IKKβ (AA) with Ser^{177} and Ser^{181} mutated to alanine had no effect on the wt c-Src-induced COX-2 promoter activity ([Fig. 5B, (c)]), but was as effective as IKKβ (Y188F) and IKKβ (Y199F) in inhibiting the *H. pylori*-induced COX-2 promoter activity [Fig. 5B, (a)].

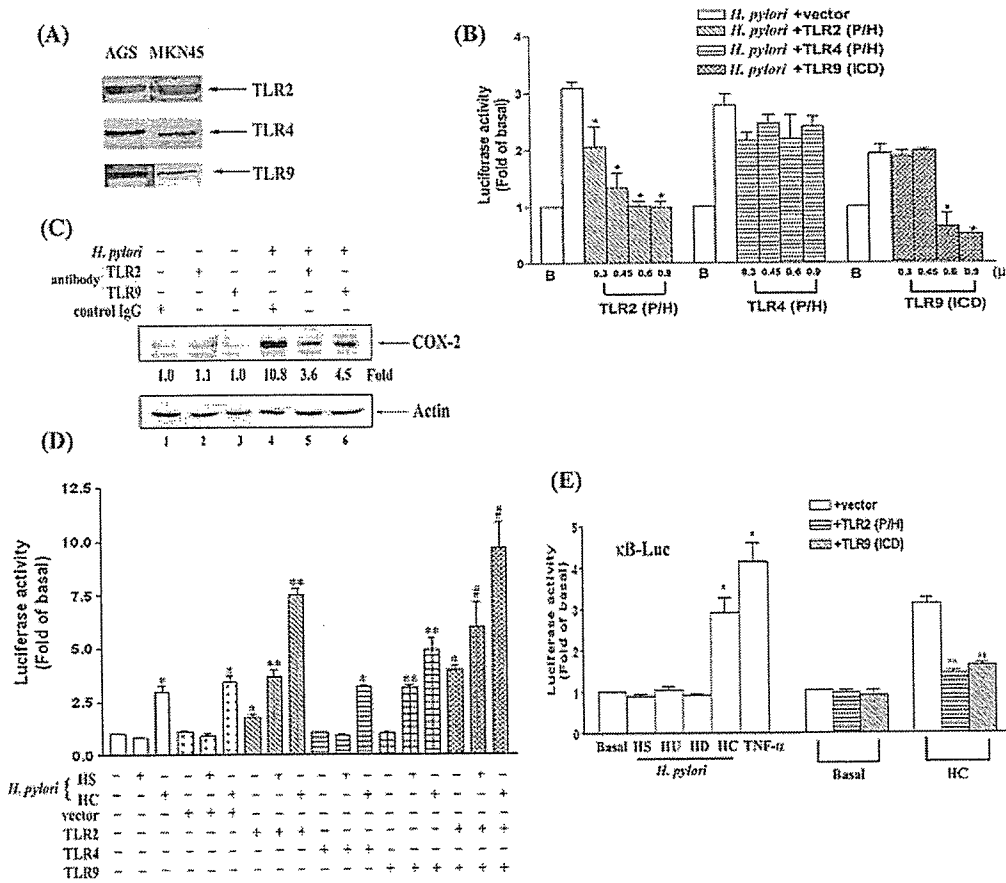

Fig. 3. Effects of TLR mutant or neutralizing antibody on COX-2 promoter activity or COX-2 expression induced by *H. pylori*. A, cell lysates were prepared and 100 μg of total proteins were subjected to Western blot analyses using anti-TLR2, TLR4, or TLR9 Ab. B and D, AGS cells were cotransfected with pGS459 and the mutant of TLR2 (P/H), TLR4 (P/H), or TLR9 (ICD) (B), or cotransfected with pGS459 and the wild-type TLR2, TLR4, TLR9, or the respective empty vector after coculture with *H. pylori* (D). E, cells were transfected with the κB-Luc plasmid, then infected with HS, HU, HD, or HC, treated with 10 ng/ml TNF-α for 6 h, or cotransfected with κB-Luc plasmid and TLR2 (P/H) or TLR9 (ICD) mutant, or the respective empty vector, then cocultured with *H. pylori* for 6 h. Luciferase activity was measured as described under *Materials and Methods*. The results were normalized to the β-galactosidase activity and expressed as the mean ± S.E. for three independent experiments performed in triplicate. *, $p < 0.05$ compared with *H. pylori* alone in B and E or with empty vector (D). **, $p < 0.05$ compared with the respective wt TLR alone. #, $p < 0.05$ compared with wt TLR2+wt TLR9 (D). C, AGS cells were incubated with anti-TLR2, TLR9, or control Ab for 3 h, then cocultured with *H. pylori* (m.o.i., 150) for 16 h. Whole-cell lysates were prepared and subjected to Western blotting using anti-COX-2 or anti-Actin Abs.

Induction of c-Src Activation by *H. pylori* Infection and the Inhibitory Effect of PI-PLC, PKC, or Src Kinase Inhibitor. To further demonstrate that the *H. pylori*-activated PKCα/c-Src/IKKβ pathway induced tyrosine phosphorylation of IKKβ, in vitro c-Src activity was measured. c-Src was isolated by immunoprecipitation using anti-c-Src Ab, and activity was measured using enolase as the substrate. As shown in Fig. 6A, the maximal c-Src activity (enolase phosphorylation) was seen after 30-min coculture with *H. pylori*, and this effect declined after 60 min (Fig. 6A, lanes 3–5). Marked autophosphorylation of c-Src was also seen (Fig. 6A). The *H. pylori*-induced c-Src activation was inhibited by 10 μM U73122, 1 μM Ro 31-8220, and PP2 at 1 and 10 μM (Fig. 6B, lanes 3–6).

Induction of IKK Activation and IκBα Degradation by *H. pylori* Infection, and the Inhibitory Effect of PI-PLC, PKC, or Src Kinase Inhibitor. Because the dominant-negative IKKα/β mutant inhibited *H. pylori*-induced COX-2 promoter activity, the endogenous IKK was immunoprecipitated with anti-IKKβ antibody, and its activity was measured. When cells were cocultured with *H. pylori* for periods of 10, 30, 60, or 120 min, a significant IKK activity was measured after 30 min [Fig. 7A, (a), lane 3] that paralleled with the degradation of IκBα [Fig. 7A, (b), lane 3]. IκBα was restored to the resting level after coculture with *H. pylori* for 24 h (data not shown). *H. pylori*-induced IKK activation was inhibited by the PI-PLC, PKC, and Src kinase inhibitors in a dose-dependent manner [Fig. 7B, (a), lanes 3–8], which was paralleled with the recovery of IκBα degradation [Fig. 7B, (b), lanes 3–8].

Involvement of c-Src-Dependent Tyrosine Phosphorylation of IKKβ by *H. pylori* Infection. Because Tyr^{188} and Tyr^{199} of IKKβ were found to be critical in the PKCα/c-Src/IKKβ pathway eliciting NF-κB activation and inducing COX-2 promoter activity (Fig. 5, A and B), the tyrosine phosphorylation of IKKβ by c-Src was examined further. c-Src was immunoprecipitated using anti-c-Src antibody, and its ability to phosphorylate IKKβ was measured using GST-IKKβ-(132–206) as an in vitro substrate. When cells were cocultured with *H. pylori*, IKKβ was phosphorylated by c-Src in a time-dependent manner; the maximal effect was seen at 30 min (Fig. 8A, lane 3), and this effect was inhibited by 1 and 10 μM PP2 (Fig. 8B, lanes 3 and 4).

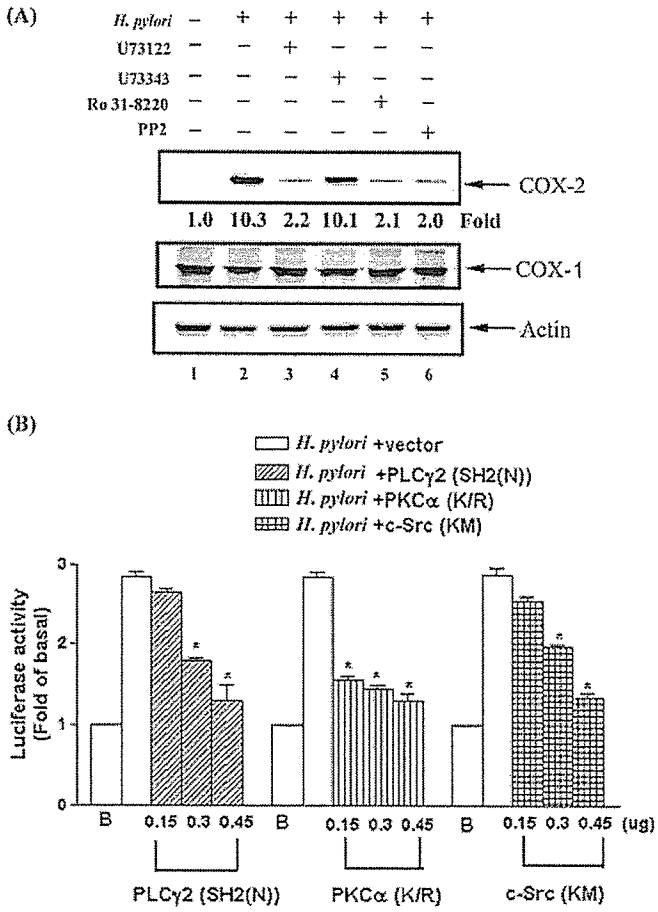

Fig. 4. Effects of various inhibitors or PLCγ2 mutant or dominant-negative mutants on *H. pylori*-induced COX-2 expression or promoter activity in AGS cells. A, cells were pretreated with U73122 (10 μM), U73343 (10 μM), Ro 31-8220 (1 μM), or PP2 (10 μM) for 30 min before coculture with *H. pylori* for 16 h. Whole-cell lysates were prepared and subjected to Western blotting using Ab specific for COX-2, COX-1, or actin. B, cells were cotransfected with pGS459 and the PLCγ2 (SH2(N)) mutant or the dominant-negative mutants of PKCα (K/R) or c-Src (KM), or the respective empty vector, then cocultured with *H. pylori* (m.o.i.,150) for 6 h. Luciferase activity was measured as described under *Materials and Methods*. The results were normalized to the β-galactosidase activity and expressed as the mean ± S.E. for three independent experiments performed in triplicate. *, $p < 0.05$ compared with *H. pylori* alone.

Discussion

In the present study, we have demonstrated different capabilities among clinical isolates of *H. pylori* to stimulate COX-2 expression in vitro. Our results demonstrated that *H. pylori* strains isolated from GC patients induced higher expression of COX-2 protein in vitro. It is likely that overexpression of COX-2 by *H. pylori* isolates from GC patients may contribute to the carcinogenesis in host induced by these strains. This phenomenon is also in agreement with the in vivo observation that COX-2 overexpression is found in 50~80% of gastric cancer patients (Sung et al., 2000; Chen et al., 2001; Wambura et al., 2002). The bacterial virulence factors and host cellular pathways of *H. pylori*-mediated COX-2 expression were further investigated.

The clinical outcome of *H. pylori* infection is determined by a complex interaction of host, environmental influences, and microbial virulence factors. The relevance of several specific *H. pylori* genes has been studied in the past. Although *cagA*, *vacA*, *iceA*, *babA2*, and *hrgA* genotypes have been reported to associate with GC (Yamaoka et al., 1998; Kidd et al., 2001; Nogueira et al., 2001; Prinz et al., 2001; Ando et al., 2002; Bravo et al., 2002), our data show no difference in these virulence genes among *H. pylori* isolates from patients with different disease statuses. The significances of VacA and CagA in *H. pylori*-induced COX-2 expression have been reported (Caputo et al., 2003; Juttner et al., 2003). Although we failed to show correlation of *cagA* and *vacA* genotypes with COX-2 expression in various clinical isolates, our data could not exclude their crucial roles in *H. pylori*-induced COX-2 expression. It is also probable that *H. pylori* might have CagA- and VacA-independent pathways to induce COX-2 expression, because all experimental strains are live bacteria and contain such toxins. The high induction of COX-2 expression by the HC strains might be exerted through other novel factors, such as γ-glutamyl transpeptidase (Busiello et al.,

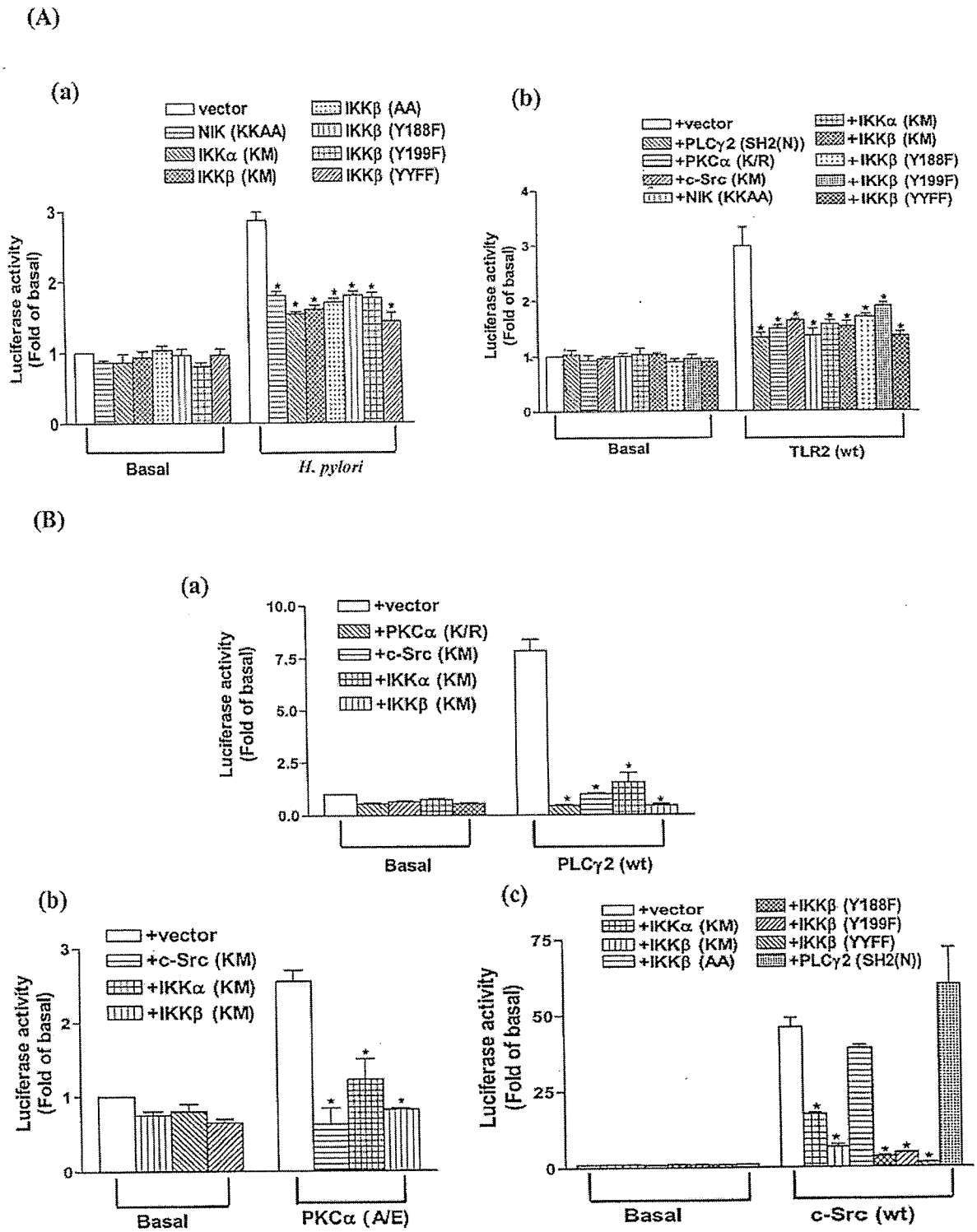

Fig. 5. Effect of PLCγ2 mutant or various dominant-negative mutants on wild-type or constitutive active plasmid-induced COX-2 promoter activity. A, (a), AGS cells were cotransfected with the dominant-negative NIK (KKAA), IKKα (KM), IKKβ (KM), IKKβ (Y188F), IKKβ (Y199F), or IKKβ (FF) mutant or the respective empty vector, then cocultured with *H. pylori* (m.o.i., 150) for 6 h. A, (b), and B, cells were cotransfected with wild-type TLR2 and PLCγ2 (SH2(N)) mutant or the dominant-negative mutants of PKCα (K/R), c-Src (KM), NIK (KKAA), IKKα (KM), IKKβ (KM), IKKβ (Y188F), IKKβ (Y199F), or IKKβ (FF) or the respective empty vector [A, (b)], or cotransfected with PLCγ2 (wt) and the dominant-negative PKCα (K/R), c-Src (KM), IKKα (KM), or IKKβ (KM) mutant [A, (a)], or cotransfected with PKCα (A/E) and the dominant-negative c-Src (KM), IKKα (KM) or IKKβ (KM) mutant [B, (b)], or cotransfected with c-Src (wt) and the PLCγ2 (SH2(N)) mutant or the dominant negative mutants of IKKα (KM), IKKβ (KM), IKKβ (AA), IKKβ (Y188F), IKKβ (Y199F), or IKKβ (FF), or the respective empty vector[B, (c)]. Luciferase activity was measured as described under *Materials and Methods*. The results were normalized to the β-galactosidase activity and expressed as the mean ± S.E. for three independent experiments performed in triplicate. *, $p < 0.05$ compared with *H. pylori* alone [A, (a)], wt TLR2 alone [A, (b)], wt PLCγ2 alone [B, (a)], PKCα (A/E) alone [B, (b)] or c-Src (wt) alone [B, (c)].

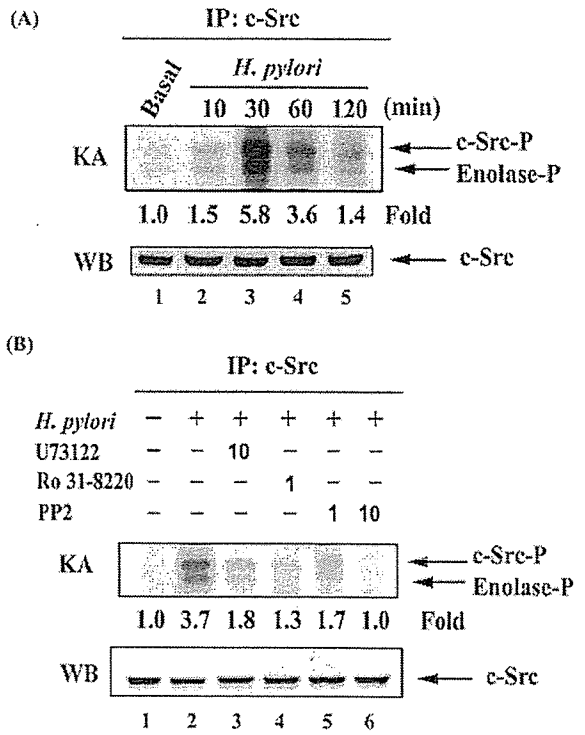

Fig. 6. Time-dependent activation of c-Src by *H. pylori* and effects of various inhibitors. AGS cells were cocultured with *H. pylori* for 10, 30, 60, or 120 min (A) or pretreated with 10 μM U73122, 1 μM Ro 31-8220, or 1 or 10 μM PP2 for 30 min before coculture with *H. pylori* for 60 min (B). Whole-cell lysates were prepared and immunoprecipitated with anti-c-Src antibody. The kinase assay (KA) and autoradiography for phosphorylated enolase were performed on the precipitates as described under *Materials and Methods*. Levels of immunoprecipitated c-Src were estimated by Western blotting (WB) using anti-c-Src antibody.

2004). It is also possible that some strains express virulence factors only at the gene level but not at the protein level. Further exploration of the molecular mechanisms involved in the enhancing effects of *H. pylori* on COX-2 expression in vitro and in vivo is warranted to provide deep insights into the role of *H. pylori* and COX-2 in the gastric carcinogenesis.

Methylation of the gene promoter DNA at the areas of CpG islands has been linked to the silencing of gene expression (Song et al., 2001). The induction of COX-2 expression in AGS cells by *H. pylori* was not through its demethylation of gene promoter, because the methylated and unmethylated status of COX-2 promoter in AGS cells was not changed after coculture with HC. Akhtar et al. (2001) also found that *H. pylori* did not change the methylation status of COX-2 promoter in AGS cells, and an increase in COX-2 protein expression was also seen after cells were cocultured with *H. pylori* (Akhtar et al., 2001) (Fig. 3C, compare lanes 1 and 2).

In addition to the methylation status, transcription factor-binding sites on the COX-2 promoter and their individual role as *cis*-acting elements regulating the transcription are of particular interest. Rodents have only one NF-κB site (−401/−393 bp in mouse), which has been shown to be involved in the TNF-α-induced COX-2 induction in a mouse osteoblast cell line (Yamamoto et al., 1995). The NF-κB-3′ site (−223/−214 bp) on the human COX-2 promoter, in concert with the NF-IL6 and CRE sites, may play a role in facilitating the induction of COX-2 by LPS and phorbol ester (Inoue et al., 1995). Our results clearly showed the indispensable role of the downstream NF-κB site (−223/−214) in TNF-α-induced COX-2 expression in human alveolar epithelial cells (Huang et al., 2003b). Our study presents the first evidence that NF-κB, NF-IL6, and CRE are involved in *H. pylori*-induced COX-2 expression. Activation of the CRE site has also been reported to be involved in the *H. pylori*-stimulated COX-2

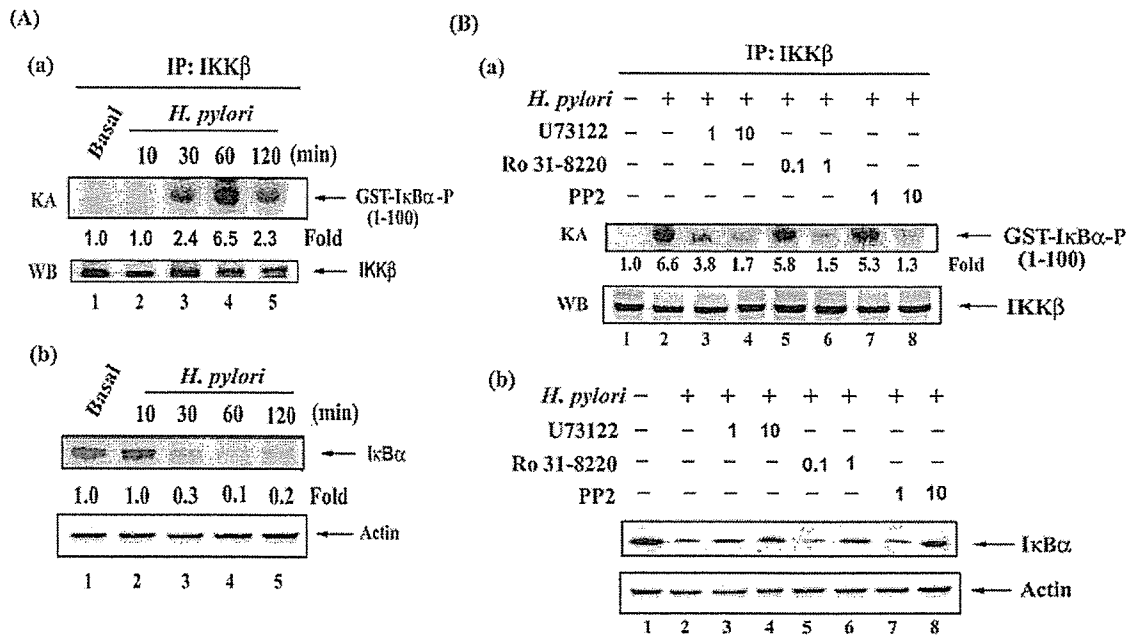

Fig. 7. Kinetics of *H. pylori*-induced IKK activation and IκB-α degradation and effects of various inhibitors. AGS cells were cocultured with *H. pylori* for 10, 30, 60, or 120 min (A) or pretreated with 1 or 10 μM U73122, 0.1 or 1 μM Ro 31-8220, or 1 or 10 μM PP2 for 30 min before coculture with *H. pylori* for 60 min (B), and then whole-cell lysates were prepared. Cell lysates were immunoprecipitated with anti-IKKβ antibody, then kinase assay (KA) and autoradiography for phosphorylated GST-IκBα (1–100) were performed on the precipitates as described under *Materials and Methods*. Levels of immunoprecipitated IKKβ protein were estimated by Western blotting (WB) using anti-IKKβ antibody [A (a) and B (a)]. Cytosolic levels of IκB-α and actin were measured using anti-IκB-α and actin antibody, respectively [A (b) and B (b)].

gene transcription (Juttner et al., 2003). However, Juttner et al. (2003) used mouse but not human COX-2 promoter construct to transfect the human AGS cells (Fig. 2). In addition to the differences in number of the NF-κB site, there are still some differences in the *cis*-acting elements on the COX-2 promoter between these two species (Inoue et al., 1995). For instance, the relative position and sequences of CRE site (5′-CGTCACGTG-3′ at −56 to −48 bp) on the mouse promoter are different from those on the human (5′-TTCGTCA-3′ at −59 to −53). Using consensus sequences containing human CRE site, we found the bindings of CREB-1, ATF-2, and c-jun to this site. TLR2 and TLR9 also initiated CRE activation (Y.-J. Chang and C.-C. Chen, unpublished data). C/EBPβ and C/EBPδ were found to bind *H. pylori*-activated NF-IL6 site (Y.-J. Chang and C.-C. Chen, unpublished data), and the involvement of TLRs in this signaling is under investigation.

All TLRs activate a common signaling pathway that culminates in the activation of NF-κB as well as the mitogen-activated protein kinases (Barton and Medzhitov, 2003). Expression of three TLRs (TLR2, TLR4, and TLR9) in both AGS and MKN45 cells was found in the present study. Although Smith et al. (2003) demonstrated the involvements of TLR2 and TLR5 in *H. pylori*-induced chemokine releases, we first revealed the roles of TLR2/9 in COX-2 induction and further explored their role in the *H. pylori*-mediated signaling pathway. Our data showed the involvements of TLR2 and TLR9 but not TLR4. When wild-type TLR was overexpressed, TLR2 and TLR9, but not TLR4, synergistically increased the *H. pylori*-induced COX-2 promoter activity. The neutralizing antibody for TLR2 or TLR9 also inhibited the *H. pylori*-induced COX-2 expression. The mutant and neutralizing antibody of TLR9 blocked the induction of *H. pylori*-mediated COX-2 promoter and expression, respectively, suggesting that *H. pylori* might mediate signaling via its CpG DNA (Hemmi et al., 2001). The finding that Gram-negative bacterial LPS stimulated TLR2 leading to NF-κB activation had been reported (Yang et al., 1998). Our data demonstrated that TLR2/9 are the major receptors mediating *H. pylori*-induced NF-κB activation leading to the COX-2 expression. This is the first report that links TLR2/9, NF-κB, and COX-2. In addition, the expression level of TLR2/9 might be a sensitive factor. HS alone did not induce COX-2 promoter activity but was enhanced in the presence of overexpression of these receptors (Fig. 3D). TLR2, but not TLR4, was also found to mediate *H. pylori*-induced NF-κB activation in MKN45 cells (Smith et al., 2003), and *Candida albicans* also acted through TLRs to activate NF-κB and induce COX-2 expression in Hela cells (Deva et al., 2003).

Because *H. pylori*-induced NF-κB activation through TLR2/TLR9 in AGS cells was demonstrated, the existence of the PKC/c-Src/IKKβ pathway downstream of TLR2/9 was examined. Several lines of evidence showed that gastric epithelial cells also exist in this pathway. First, both *H. pylori*- and wt TLR2-induced COX-2 promoter activities were inhibited by the dominant-negative tyrosine mutants IKKβ (Y188F), IKKβ (Y199F), or IKKβ (FF). Second, wt c-Src-

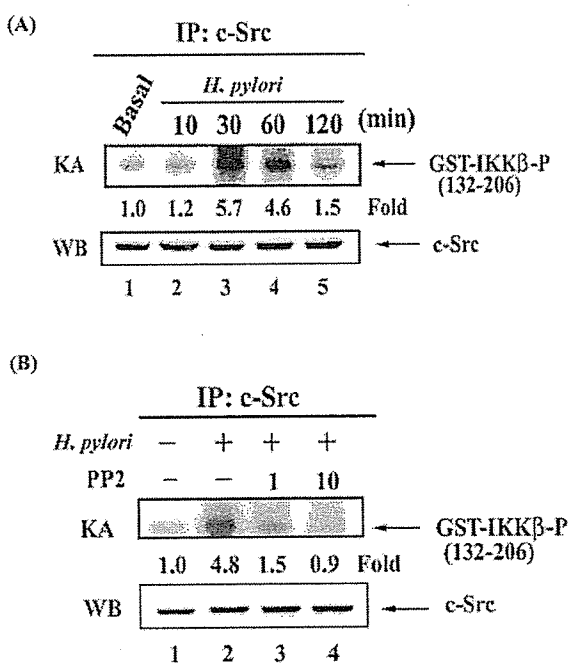

Fig. 8. c-Src-dependent phosphorylation of IKKβ induced by *H. pylori* and the inhibition by PP2. AGS cells were cocultured with *H. pylori* for 10, 30, 60, or 120 min (A) or pretreated with 1 or 10 μM PP2 for 30 min before coculture with *H. pylori* for 60 min (*B*). Whole-cell lysates were prepared and immunoprecipitated with anti-c-Src antibody, then kinase assay (KA) and autoradiography were performed for phosphorylated GST-IKKβ (132–206). The amount of immunoprecipitated c-Src was detected by Western blotting (WB) using anti-c-Src antibody.

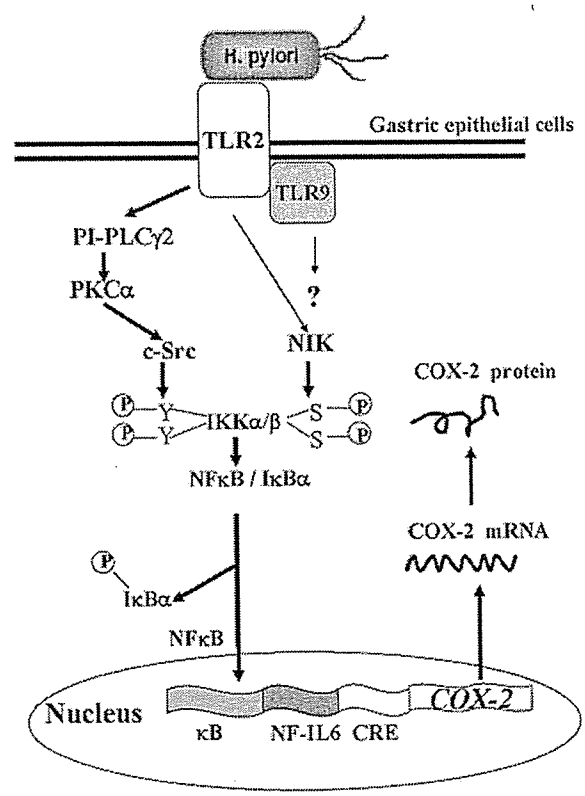

Fig. 9. Schematic representation of the signaling pathways involved in *H. pylori*-induced COX-2 expression in the AGS epithelial cells. The κB, NF-IL6, and CRE elements are involved in *H. pylori*-induced COX-2 expression. *H. pylori* acts through TLR2 and TLR9, then activates PI-PLCγ to induce PKCα and c-Src activation, leading to tyrosine phosphorylation of IKKα/β. *H. pylori* also activates NIK, leading to serine phosphorylation of IKKα/β. These two pathways converge at IKKα/β, resulting in the phosphorylation and degradation of IκBα, stimulation of NF-κB in the COX-2 promoter, and finally initiation of COX-2 expression.

induced COX-2 promoter activity was inhibited by the dominant-negative tyrosine mutants but not by the IKKβ (AA) mutant, in which Ser^{177} and Ser^{181} are mutated. Third, *H. pylori* induced c-Src activation as well as IKK activation and IκBα degradation, and the PI-PLC, PKC, and Src inhibitors inhibited these effects. Fourth, an in vitro kinase assay demonstrated that *H. pylori*-stimulated c-Src phosphorylates IKKβ at Tyr^{188} and Tyr^{199}, and this effect was inhibited by PP2. It is already known that these two tyrosine residues in IKKβ are conserved with other Ser/Thr kinases such as Akt1 and PKCδ (Huang et al., 2003a,b). Therefore, two signal pathways are involved in the *H. pylori*-induced NF-κB activation leading to COX-2 expression. One is the activation of NIK/IKK pathway, which was already recognized (Malinin et al., 1997), and the other is the activation of PKC-dependent c-Src pathway demonstrated here. These two pathways converge at IKKα/β. The PKC/c-Src/IKK pathway, shown to be involved in the induction of COX-2 expression here, might be a common pathway for the inducible gene expression, because the TNF-α-, IL-1β-, and IFN-γ-induced COX-2 or ICAM-1 expression in lung epithelial cells also involved the PKC-dependent activation of c-Src (Chang et al., 2002, 2004; Huang et al., 2003a,b). Although the *H. pylori*-up-regulated COX-2 mRNA expression and PGE2 synthesis were already found (Romano et al., 1998), we are the first to identify the involvement of NF-κB, NF-IL6, and CRE sites in *H. pylori*-induced COX-2 expression and to further explore the existence of a novel TLR2/9/c-Src/NF-κB/COX-2 pathway.

In summary, the identification of clinical isolates of *H. pylori* from GC patients induced high levels of COX-2 expression in vitro. Although the genetic bases for this phenomenon are not known at present, these clinical isolates may represent a group of *H. pylori* strains harboring novel virulence factors that could be pursued in the future. The involvement of NF-κB, NF-IL6, and CRE sites in the regulation of *H. pylori*-induced COX-2 expression are demonstrated. The mechanism of TLR2/TLR9 mediated *H. pylori*-induced NF-κB activation is further examined. *H. pylori* acts through the TLR2/TLR9 to activate both the PI-PLCγ/PKCα/c-Src/IKKα/β and NIK/IKKα/β pathways, resulting in the phosphorylation and degradation of IκBα, which in turn leads to the stimulation of NF-κB and COX-2 gene expression. A schematic presentation of the involvements of these pathways in the AGS cells is shown in Fig. 9. This COX-2 expression may contribute to the carcinogenesis in patients colonized with these cancer strains.

References

Akhtar M, Cheng Y, Magno RM, Ashktorab H, Smoot DT, Meltzer SJ, and Wilson KT (2001) Promoter methylation regulates *Helicobacter pylori*-stimulated cyclooxygenase-2 expression in gastric epithelial cells. *Cancer Res* **61**:2399–2403.

Ando T, Wassenaar TM, Peek RM Jr, Aras RA, Tschumi AI, van Doorn LJ, Kusugami K, and Blaser MJ (2002) A *Helicobacter pylori* restriction endonuclease-replacing gene, hrgA, is associated with gastric cancer in Asian strains. *Cancer Res* **62**:2385–2389.

Barton GM and Medzhitov R (2003) Toll-like receptor signaling pathways. *Science (Wash DC)*. **300**:1524–1525.

Blaser MJ (2002) Polymorphic bacteria persisting in polymorphic hosts: assessing *Helicobacter pylori*-related risks for gastric cancer. *J Natl Cancer Inst* **94**:1662–1663.

Bodger K and Crabtree JE (1998) *Helicobacter pylori* and gastric inflammation. *Br Med Bull* **54**:139–150.

Bravo LE, van Doom LJ, Reakpe JL, and Correa P (2002) Virulence associated genotypes of *Helicobacter pylori*: do they explain the African enigma? *Am J Gastroenterol* **97**:2839–2842.

Busiello I, Acquaviva R, Di Popolo A, Blanchard TG, Ricci V, Romano M, and Zarrilli R (2004) *Helicobacter pylori* gamma-glutamyltranspeptidase upregulates COX-2 and EGF-related peptide expression in human gastric cells. *Cell Microbiol* **6**:255–267.

Caputo R, Tuccillo C, Manzo BA, Zarrilli R, Tortora G, Blanco Cdel V, Ricci V, Ciardiello F, and Romano M (2003) *Helicobacter pylori* VacA toxin up-regulates vascular endothelial growth factor expression in MKN 28 gastric cells through an epidermal growth factor receptor-, cyclooxygenase-2-dependent mechanism. *Clin Cancer Res* **9**:2015–2021.

Chang YJ, Holtzman MJ, and Chen CC (2002) Interferon-γ-induced epithelial ICAM-1 expression and monocyte adhesion. Involvement of protein kinase C-dependent c-Src tyrosine kinase activation pathway. *J Biol Chem* **277**:7118–7126.

Chang YJ, Holtzman MJ, and Chen CC (2004) Differential role of Janus family kinases (JAKs) in interferon-γ-induced lung epithelial ICAM-1 expression: involving protein interactions between JAKs, phospholipase Cγ, c-Src, and STAT1. *Mol Pharmacol* **65**:589–598.

Chen CN, Sung CT, Lin MT, Lee PH, and Chang KJ (2001) Clinicopathologic association of cyclooxygenase 1 and cyclooxygenase 2 expression in gastric adenocarcinoma. *Ann Surg* **233**:183–188.

Deva R, Shankaranarayanan P, Ciccoli R, and Nigam S (2003) Candida albicans induces selectively transcriptional activation of cyclooxygenase-2 in HeLa cells: pivotal roles of Toll-like receptors, p38 mitogen-activated protein kinase and NF-kappa B. *J Immunol.* **171**:3047–3055.

Hemmi H, Takeuchi O, Kawai T, Kaisho T, Sato S, Sanjo H, Matsumoto M, Hoshino K, Wagner H, Takeda K, et al. (2000) A Toll-like receptor recognizes bacterial DNA. *Nature (Lond)* **408**:740–745.

Huang WC, Chen JJ, and Chen CC (2003a) c-Src-dependent tyrosine phosphorylation of IKKβ is involved in tumor necrosis factor-α-induced intercellular adhesion molecule-1 expression. *J Biol Chem* **278**:9944–9952.

Huang WC, Chen JJ, Inoue H, and Chen CC (2003b) Tyrosine phosphorylation of I-κB kinase α/β by protein kinase C-dependent c-Src activation is involved in TNF-α-induced cyclooxygenase-2 expression. *J Immunol* **170**:4767–4775.

Inoue H, Yokoyama C, Hara S, Tone Y, and Tanabe T (1995) Transcriptional regulation of human prostaglandin-endoperoxide synthase-2 gene by lipopolysaccharide and phorbol ester in vascular endothelial cells. Involvement of both nuclear factor for interleukin-6 expression site and cAMP response element. *J Biol Chem* **270**:24965–24971.

Jackson LM, Wu KC, Mahida YR, Jenkins D, and Hawkey CJ (2000) Cyclooxygenase 1 and 2 in normal, inflamed and ulcerated human gastric mucosa. *Gut* **47**:762–770.

Juttner S, Cramer T, Wessler S, Walduck A, Gao F, Schmitz F, Wunder C, Weber M, Fischer SM, Schmidt WE, et al. (2003) *Helicobacter pylori* stimulates host cyclooxygenase-2 gene transcription: critical importance of MEK/ERK-dependent activation of USF1/-2 and CREB transcription factors. *Cell Microbiol* **5**:821–834.

Keates S, Hitti YS, Upton M, and Kelly CP (1997) *Helicobacter pylori* infection activates NF-kappa B in gastric epithelial cells. *Gastroenterology* **113**:1099–1109.

Kidd M, Peek RM, Lastovica AJ, Israel DA, Kummer AF, and Louw JA (2001) Analysis of iceA genotypes in South African *Helicobacter pylori* strains and relationship to clinically significant disease. *Gut* **49**:629–635.

Kosaka T, Miyata A, Ihara H, Hara S, Sugimoto T, Takeda O, Takahashi E, and Tanabe T (1994) Characterization of the human gene (PTGS2) encoding prostaglandin-endoperoxide synthase 2. *Eur J Biochem.* **221**:889–897.

Malinin NL, Boldin MP, Rovalenko AV, and Wallach D (1997) MAP3K-related kinase involved in NF-κB induction by TNF, CD95 and IL-1. *Nature (Lond)* **385**:540–544.

Muta T and Takeshige K (2001) Essential roles of CD14 and lipopolysaccharide-binding protein for activation of toll-like receptor (TLR)2 as well as TLR4 Reconstitution of TLR2- and TLR4-activation by distinguishable ligands in LPS preparations. *Eur J Biochem* **268**:4580–4589.

Nogueira C, Figueiredo C, Carneiro F, Gomes AT, Barreira R, Figueira P, Salgado C, Belo L, Peixoto A, Bravo JC, et al. (2001) *Helicobacter pylori* genotypes may determine gastric histopathology. *Am J Pathol* **158**:647–654.

Parsonnet J, Friedman GD, Vandersteen DP, Chang Y, Vogelman JH, Orentreich N, and Sibley RK (1991) *Helicobacter pylori* infection and the risk of gastric carcinoma. *N Engl J Med* **325**:1127–1131.

Passaro DJ, Chosy EJ, and Parsonnet J (2002) *Helicobacter pylori*: consensus and controversy. *Clin Infect Dis* **35**:298–304.

Peek RM and Blaser MJ (2002) *Helicobacter pylori* and gastrointestinal tract adenocarcinomas. *Nat Rev Cancer* **2**:28–37.

Poltorak A, He X, Smirnova I, Liu MY, Van Huffel C, Du X, Birdwell D, Alejos E, Silva M, Galanos C, et al. (1998) Defective LPS signaling in C3H/Hel and C57BL/10ScCr mice: mutation in TLR4 gene. *Science (Wash DC)* **282**:2085–2088.

Prinz C, Schoniger M, Rad R, Becker I, Keiditsch E, Wagenpfeil S, Classen M, Rosch T, Schepp W, and Gerhard M (2001) Key importance of the *Helicobacter pylori* adherence factor blood group antigen binding adhesin during chronic gastric inflammation. *Cancer Res* **61**:1903–1909.

Rock FL, Hardiman G, Timans JC, Kastelein RA, and Bazan JF (1998) A family of human receptors structurally related to *Drosophila* Toll. *Proc Natl Acad Sci* **95**:588–593.

Romano M, Ricci V, Memoli A, Tuccillo C, Di Popolo A, Sommi P, Acquaviva AM, Del Vecchio Blanco C, Bruni CB, and Zarrilli R (1998) *Helicobacter pylori* up-regulates cyclooxygenase-2 mRNA expression and prostaglandin E2 synthesis in MKN 28 gastric mucosal cells in vitro. *J Biol Chem* **273**:28560–28563.

Sheu BS, Sheu SM, Yang HB, Huang AH, and Wu JJ (2003) Host gastric Lewis expression determines the bacterial density of *Helicobacter pylori* in babA2 genopositive infection. *Gut* **52**:927–932.

Smith MF Jr, Mitchell A, Li G, Ding S, Fitzmaurice AM, Ryan K, Crowe S, and Goldberg JB (2003) Toll-like receptor (TLR) 2 and TLR5, but not TLR4, are required for *Helicobacter pylori*-induced NF-κB activation and chemokine expression by epithelial cells. *J Biol Chem* **278**:32552–32560.

Song SH, Jong HS, Choi HH, Inoue H, Tanabe T, Kim NK, and Bang YJ (2001) Transcriptional silencing of Cyclooxygenase-2 by hyper-methylation of the 5′ CpG island in human gastric carcinoma cells. *Cancer Res* **61**:4628–4635.

Sung JJ, Leung WK, Go MY, To KF, Cheng AS, Ng EK, and Chan FK (2000)

Cyclooxygenase-2 expression in *Helicobacter pylori*-associated premalignant and malignant gastric lesions. *Am J Pathol* **157**:729–735.

Takahashi S, Fujita T, and Yamamoto A (2000) Role of cyclooxygenase-2 in *Helicobacter pylori*- induced gastritis in Mongolian gerbils. *Am J Physiol* **279**:G791–G798.

Takeshita F, Leifer CA, Gursel I, Ishii KJ, Takeshita S, Gursel M, and Klinman DM (2001) Role of Toll-like receptor 9 in CpG DNA-induced activation of human cells. *J Immunol* **167**:3555–3558.

Takeuchi O, Hoshino K, Kawai T, Sanjo H, Takada H, Ogawa T, Takeda K, and Akira S (1999) Differential role of TLR2 and TLR4 in recognition of gram-negative and gram-positive bacteria cell wall components. *Immunity* **11**:443–451.

van Rees BP, Saukkonen K, Ristimaki A, Polkowski W, Tytgat GN, Drillenburg P, and Offerhaus GJ (2002) Cyclooxygenase-2 expression during carcinogenesis in the human stomach. *J Pathol* **196**:171–199.

Wambura C, Aoyama N, Shirasaka D, Sakai T, Ikemura T, Sakashita M, Maekawa S, Kuroda K, Inoue T, Ebara S, et al. (2002) Effect of *Helicobacter pylori*-induced cyclooxygenase-2 on gastric epithelial cell kinetics: implication for gastric carcinogenesis. *Helicobacter* **7**:129–138.

Wang HJ, Kuo CH, Yeh AM, Chang CL, and Wang WC (1998) Vacuolating toxin production in clinical isolates of *Helicobacter pylori* with different vacA genotypes. *J Infect Dis* **178**:207–212.

Yamamoto K, Arakawa T, Ueda N, and Yamamoto S (1995) Transcriptional roles of NF-κB and NF-IL6 in the TNA-α-dependent induction of cyclooxygenase-2 in MC3T3-E1 cells. *J Biol Chem* **270**:31315-31320.

Yamaoka Y, Kodama T, Kashima K, Graham DY, and Sepulveda AR (1998) Variants of the 3′ region of the cagA gene in *Helicobacter pylori* isolates from patients with different *H. pylori*-associated diseases. *J Clin Microbiol* **36**:2258–2263.

Yang RB, Mark MR, Gray A, Huang A, Xie MH, Zhang M, Goddard A, Wood WI, Gurney AL, and Godowski PJ (1998) Toll-like receptor-2 mediates lipopolysaccharide-induced cellular signalling. *Nature (Lond)* **395**:284–288.

Address correspondence to: Dr. Ching-Chow Chen, Department of Pharmacology, College of Medicine, National Taiwan University, No.1, Jen-Ai Road, 1st Section, Taipei 10018, Taiwan. E-mail: ccchen@ha.mc.ntu.edu.tw

Bradykinin B2 Receptor Mediates NF-κB Activation and Cyclooxygenase-2 Expression via the Ras/Raf-1/ERK Pathway in Human Airway Epithelial Cells[1]

Bing-Chang Chen,* Chung-Chi Yu,† Hui-Chieh Lei,† Ming-Shyan Chang,‡ Ming-Jen Hsu,† Chuen-Lin Huang,† Mei-Chieh Chen,§ Joen-Rong Sheu,‡ Tseng-Fu Chen,‡ Ta-Liang Chen,¶ Hiroyasu Inoue,‖ and Chien-Huang Lin*†

In this study, we investigated the signaling pathways involved in bradykinin (BK)-induced NF-κB activation and cyclooxygenase-2 (COX-2) expression in human airway epithelial cells (A549). BK caused concentration- and time-dependent increase in COX-2 expression, which was attenuated by a selective B2 BK receptor antagonist (HOE140), a Ras inhibitor (manumycin A), a Raf-1 inhibitor (GW 5074), a MEK inhibitor (PD 098059), an NF-κB inhibitor (pyrrolidine dithiocarbate), and an IκB protease inhibitor (L-1-tosylamido-2-phenylethyl chloromethyl ketone). The B1 BK receptor antagonist (Lys-(Leu^8)des-Arg^9-BK) had no effect on COX-2 induction by BK. BK-induced increase in COX-2-luciferase activity was inhibited by cells transfected with the κB site deletion of COX-2 construct. BK-induced Ras activation was inhibited by manumycin A. Raf-1 phosphorylation at Ser^{338} by BK was inhibited by manumycin A and GW 5074. BK-induced ERK activation was inhibited by HOE140, manumycin A, GW 5074, and PD 098059. Stimulation of cells with BK activated IκB kinase αβ (IKKαβ), IκBα phosphorylation, IκBα degradation, p65 and p50 translocation from the cytosol to the nucleus, the formation of an NF-κB-specific DNA-protein complex, and κB-luciferase activity. BK-mediated increase in IKKαβ activity and formation of the NF-κB-specific DNA-protein complex were inhibited by HOE140, a Ras dominant-negative mutant (RasN17), manumycin A, GW 5074, and PD 098059. Our results demonstrated for the first time that BK, acting through B2 BK receptor, induces activation of the Ras/Raf-1/ERK pathway, which in turn initiates IKKαβ and NF-κB activation, and ultimately induces COX-2 expression in human airway epithelial cell line (A549). *The Journal of Immunology,* 2004, 173: 5219–5228.

Bradykinin (BK)[3] is rapidly generated following inflammation or injury (1). The release of BK is known to mediate multiple proinflammatory effects including smooth muscle contraction, vasodilation, increased vascular permeability, eicosanoid synthesis, and neuropeptide release (1, 2). Furthermore, BK has been shown to play a critical role in the development of airway hyperresponsiveness in experimental models of airway inflammation (3–5). To elucidate the role of BK in this process, we assessed the effect of BK on cyclooxygenase-2 (COX-2) expression in human airway epithelial cells.

COX is the key enzyme to synthesize PGs and thromboxane from arachidonic acid (6). Two COX isozymes, COX-1 and COX-2, have been cloned and identified to have 60% homology in humans (7, 8). COX-1, which is constitutively expressed in most tissues, mediates physiological responses and regulates renal and vascular homeostasis. The second COX isoform, COX-2, is considered to be an inducible immediate-early gene product whose synthesis in cells can be up-regulated by mitogenic or inflammatory stimuli including TNF-α, IL-1β, lipoteichoic acid, and LPS (9–12). COX-2 is thought to be responsible for the production of proinflammatory PGs in various models of inflammation (13). Previous studies have shown that BK can induce COX-2 expression in human airway smooth muscle cells and fibroblasts (14, 15). However, the expression of COX-2 induced by BK in human airway epithelial cell has not been determined, and the signal transduction events, especially the Ras/Raf-1/ERK pathway, leading to the expression of COX-2 by BK are unclear.

Several G protein-couple receptors, including the B2 BK receptor, have been shown to mediate NF-κB activation and cytokine gene transcription in human epithelial cells and fibroblasts (16, 17). BK-stimulated NF-κB activation has been demonstrated to be mediated through B2 BK receptors coupled to the G_i/G_o class of heterotrimeric G proteins (16). Activation of the small GTP-binding protein, Rho A, and PI3K are involved in BK-stimulated NF-κB activation in A549 cells (17, 18). BK has also been reported to activate the small GTP-binding proteins, Cdc42 and Rac1, stimulating the formation of peripheral actin microspikes and membrane ruffling in Swiss 3T3 fibroblasts (19). Moreover, BK was shown to activate Ras in PC-12 rat adrenal pheochromocytoma cells and inner medullary collecting duct cells (20, 21). However, little information is available about the role of Ras in the regulation of NF-κB activation and COX-2 expression following BK stimulation.

*School of Respiratory Therapy, †Graduate Institutes of Biomedical Technology, ‡Graduate Institutes of Medical Sciences, §Department of Microbiology and Immunology, College of Medicine, Taipei Medical University, Taipei, Taiwan; ¶Department of Anesthesiology, Taipei Medical University-Wan Fang Hospital, Taipei, Taiwan; and ‖Department of Pharmacology, National Cardiovascular Center Research Institute, Osaka, Japan

Received for publication March 18, 2004. Accepted for publication August 13, 2004.

The costs of publication of this article were defrayed in part by the payment of page charges. This article must therefore be hereby marked *advertisement* in accordance with 18 U.S.C. Section 1734 solely to indicate this fact.

[1] This work was supported by grants from the National Science Council of Taiwan (NSC 92-2314-B-038-059 and NSC 93-2314-B-038-014).

[2] Address correspondence and reprint requests to Dr. Chien-Huang Lin, School of Respiratory Therapy, Taipei Medical University, 250 Wu-Hsing Street, Taipei 110, Taiwan. E-mail address: chlin@tmu.edu.tw

[3] Abbreviations used in this paper: BK, bradykinin; COX-2, cyclooxygenase-2; IKKαβ, IκB kinase αβ; PDTC, pyrrolidine dithiocarbate; Raf-1 RBD, Ras-binding domain for Raf-1; TPCK, L-1-tosylamido-2-phenylethyl chloromethyl ketone.

Copyright © 2004 by The American Association of Immunologists, Inc.

0022-1767/04/$02.00

Ras has been found to couple with multiple effector systems to activate distinct physiological and pathological responses such as cell proliferation and proinflammatory mediator release (22, 23). An important class of Ras effectors is the MAPK family. The classic Ras-mediated pathway involves the binding of Raf-1 and subsequent phosphorylation of Raf-1 at Ser^{338} by many kinases (24, 25), which in turn activates ERKs (26), and consequently phosphorylates many target proteins including transcription factors and protein kinases (27). A role for Ras in COX-2 induction has been implied in many cell types (21, 23). However, the role of the Ras/Raf-1/ERK pathway in BK-induced COX-2 expression has not been investigated in human airway epithelial cells (A549). This study was intended to identify the role of the Ras/Raf-1/ERK pathway in BK-mediated NF-κB activation and COX-2 expression in A549 cells. Our hypothesis is that BK might activate the Ras/Raf-1/ERK pathway, which in turn induces IκB kinase αβ (IKKαβ) and NF-κB activation, and ultimately causes COX-2 expression in A549 cells.

Materials and Methods

Materials

Manumycin A, PD 098059, and SB 203580 were obtained from Calbiochem (San Diego, CA). DMEM/Ham's F-12, FCS, penicillin/streptomycin, and Lipofectamine plus were purchased from Invitrogen Life Technologies (Gaithersburg, MD). Specific Abs for α-tubulin and COX-2 were purchased from Transduction Laboratories (Lexington, KY). Protein A/G beads, IκBα protein (aa 1~317), specific Abs for ERK2, ERK phosphorylated at Tyr^{204}, IκBα, IκBα phosphorylated at Ser^{32}, IKKα, IKKβ, Raf-1, and anti-mouse and anti-rabbit IgG-conjugated HRP were purchased from Santa Cruz Biotechnology (Santa Cruz, CA). A specific Ab for Raf-1 phosphorylated at Ser^{338} was purchased from Cell Signaling and Neuroscience (St. Louis, MO). Anti-mouse and anti-rabbit IgG-conjugated alkaline phosphatases were purchased from Jackson ImmunoResearch Laboratories (West Grove, PA). pGL2-ELAM-Luc (which is under the control of one NF-κB binding site) and pBK-CMV-Lac Z were kindly provided by Dr. W.-W. Lin (National Taiwan University, Taipei, Taiwan). A Ras dominant-negative mutant (RasN17) and a Ras activity assay kit were purchased from Upstate Biotechnology (Lake Placid, NY). [γ-^{32}P]ATP (6000 Ci/mmol) was purchased from Amersham (Buckinghamshire, U.K.). All materials for SDS-PAGE were purchased from Bio-Rad (Hercules, CA). All other chemicals were obtained from Sigma-Aldrich (St. Louis, MO).

Cell culture

A549 cells, a human pulmonary epithelial carcinoma cell line with type II alveolar epithelial cell differentiation, was obtained from American Type Culture Collection (Manassas, VA) and grown in DMEM/Ham's F-12 nutrient mixture containing 10% FCS, 50 U/ml penicillin G, and 100 μg/ml streptomycin in a humidified 37°C incubator. After reaching confluence, cells were seeded onto 10-cm dishes for EMSA, 6-cm dishes for immunoblotting or kinase assays, or 12-well plates for transfection and κB-luciferase assays.

Immunoblot analysis

To determine the expression of COX-2, α-tubulin, ERK phosphorylation at Tyr^{204}, ERK2, IKKαβ, IκBα phosphorylation at Ser^{32}, IκBα, Ras, Raf-1 phosphorylation at Ser^{338}, and Raf-1 in A549 cells, proteins were extracted and Western blot analysis was performed as described previously (12). Briefly, A549 cells were cultured in 6-cm dishes. After reaching confluence, cells were treated with vehicle, BK, or pretreated with specific inhibitors as indicated, followed by BK. After incubation, cells were washed twice in ice-cold PBS and solubilized in extraction buffer containing 10 mM Tris (pH 7.0), 140 mM NaCl, 2 mM PMSF, 5 mM DTT, 0.5% Nonidet P-40, 0.05 mM pepstatin A, and 0.2 mM leupeptin. Samples of equal amounts of protein (60 μg) were placed on SDS-PAGE, transferred onto a PVDF membrane and then incubated in TBST buffer (150 mM NaCl, 20 mM Tris-HCl, 0.02% Tween 20 (pH 7.4)) containing 5% nonfat milk. Proteins were visualized by specific primary Abs and then incubated with HRP- or alkaline phosphatase-conjugated second Abs. Immunoreactivity was detected using ECL or NBT/5-bromo-4-chloro-3-indolyl phosphate following the manufacturer's instructions. Quantitative data were obtained using a computing densitometer with scientific imaging systems (Kodak, Rochester, NY).

Preparation of nuclear extracts and the EMSA

A549 cells were cultured in 10-cm dishes. After reaching confluence, cells were treated with vehicle or 10 nM BK for various time intervals, and then cells were scraped and collected. In some experiments, cells were pretreated with specific inhibitors as indicated or transfected with the Ras dominant-negative mutant (RasN17) for 24 h before BK treatment. The cytosolic and nuclear protein fractions were then separated as described previously (28). Briefly, cells were washed with ice-cold PBS, and pelleted. Cell pellets were resuspended in hypotonic buffer (10 mM HEPES (pH 7.9), 10 mM KCl, 0.5 mM DTT, 10 mM aprotinin, 10 mM leupeptin, and 20 mM PMSF) for 15 min on ice, and vortexed for 10 s. Nuclei were pelleted by centrifugation at 15,000 × *g* for 1 min. Supernatants containing cytosolic proteins were collected. A pellet containing nuclei was resuspended in hypertonic buffer (20 mM HEPES (pH 7.6), 25% glycerol, 1.5 mM $MgCl_2$, 4 mM EDTA, 0.05 mM DTT, 10 mM aprotinin, 10 mM leupeptin, and 20 mM PMSF) for 30 min on ice. Supernatants containing nuclear proteins were collected by centrifugation at 15,000 × *g* for 2 min and then stored at −70°C. The protein levels of p65 and p50 NF-κB in the cytosolic and nuclear fractions, and IκBα phosphorylated at Ser^{32} and IκBα in the cytosolic fractions were determined by Western blot analysis performed as described.

A double-stranded oligonucleotide probe containing NF-κB sequences (5′-AGTTGAGGGGACTTTCCCAGGC-3′; Promega, Madison, WI) was purchased and end labeled with [γ-^{32}P]ATP using T4 polynucleotide kinase. The nuclear extract (2.5~5 μg) was incubated with 1 ng of a ^{32}P-labeled NF-κB probe (50,000~75,000 cpm) in 10 μl of binding buffer containing 1 μg poly(dI-dC), 15 mM HEPES (pH 7.6), 80 mM NaCl, 1 mM EDTA, 1 mM DTT, and 10% glycerol at 30°C for 25 min. DNA-nuclear protein complexes were separated from the DNA probe by electrophoresis on 5% polyacrylamide gels. Gels were vacuum-dried and subjected to autoradiography with an intensifying screen at −80°C.

Transfection and κB- or COX-2-luciferase assays

For these assays, 2 × 10^5 A549 cells were seeded onto 12-well plates, and transfected in the following day using Lipofectamine plus (Invitrogen Life Technologies) with 0.5 μg of pGL2-ELAM-Luc, human COX-2 promoter-luciferase (−327/+59), or the κB site (−223/−214) deletion mutant of COX-2 (κBM), plus 1 μg of pBK-CMV-Lac Z. After 24 h, the medium was aspirated and replaced by fresh DMEM/Ham's F12 containing 10% FBS. Cells were stimulated with 10 nM BK for another 24 h before harvest. Luciferase activity was determined by a luciferase assay system (Promega), and was normalized on the basis of Lac Z expression. The level of induction of luciferase activity was compared as a ratio of cells with and without stimulation.

Immunoprecipitation and IKKαβ activity assay

A549 cells were grown in 6-cm dishes. After reaching confluence, cells were either treated with 10 nM BK for the indicated time intervals, pretreated with specific inhibitors as indicated, or transfected with the Ras dominant-negative mutant (RasN17) for 24 h followed by BK treatment. After incubation, cells were washed twice with ice-cold PBS, lysed in 1 ml of lysis buffer containing 20 mM Tris-HCl (pH 7.5), 1 mM $MgCl_2$, 125 mM NaCl, 1% Triton X-100, 1 mM PMSF, 10 μg/ml leupeptin, 10 μg/ml aprotinin, 25 mM β-glycerophosphate, 50 mM NaF, and 100 μM sodium orthovanadate, and centrifuged. The supernatant was then immunoprecipitated with polyclonal Abs against IKKα or IKKβ in the presence of A/G-agarose beads overnight. The beads were washed three times with lysis buffer and two times with kinase buffer containing 20 mM HEPES (pH 7.4), 20 mM $MgCl_2$, and 2 mM DTT. The kinase reactions were performed by incubating immunoprecipitated beads with 20 μl of kinase buffer supplemented with 20 μM ATP, 0.5 μg of GST-IκBα protein (aa 1~317), and 3 μCi of [γ-^{32}P]ATP at 30°C for 30 min. The reaction mixtures were analyzed by 12% SDS-PAGE followed by autoradiography.

Ras activity assay

Ras activity was measuring by using a Ras activity assay kit. The assay was performed according to the manufacturer's instructions. Briefly, cells were washed twice with ice-cold PBS, lysed in magnesium lysis buffer (25 mM HEPES (pH 7.5), 150 mM NaCl, 5% Igepal CA-630 (Upstate Biotechnology, Lake Placid, NY), 10 mM $MgCl_2$, 5 mM EDTA, 10% glycerol, 10 μg/ml aprotinin, and 10 μg/ml leupeptin), and centrifuged. An equal volume of lysate was incubated with 5 μg of Ras-binding domain for Raf-1 (Raf-1 RBD) at 4°C overnight, and beads were washed three times with magnesium lysis buffer. Bound Ras proteins were then solubilized in 2× Laemmli sample buffer and quantitatively detected by Western blotting

(10% SDS-PAGE) using mouse monoclonal Ras with the ECL system, and by densitometry of corresponding bands using scientific imaging systems.

Statistical analysis

Results are presented as the mean ± SE from at least three independent experiments. One-way ANOVA followed by, when appropriate, Bonferroni's multiple-range test was used to determine the statistical significance of the difference between means. A p-value of <0.05 was considered statistically significant.

Results

BK induces COX-2 expression in A549 cells

Human airway epithelial cells (A549) were chosen to investigate the signal pathways of BK in COX-2 expression, an inflammatory response gene. Treatment with BK (0.1~1000 nM) for 4 h induced COX-2 protein expression in a concentration-dependent manner, with a maximum effect at 10 nM BK treatment (Fig. 1*A*); this induction occurred in a time-dependent manner (Fig. 1*B*). After treatment, COX-2 protein bands began to appear at 2 h, reached a maximum at 4 h, and gradually diminished from 8 to 24 h. After 4 h of treatment with 10 nM BK, the COX-2 protein had increased by ~246 ± 34% (Fig. 1*B*). Two types of BK receptors have been defined and cloned: B1 and B2 BK receptors (29). The receptor specificity of BK-mediated COX-2 expression was therefore tested using specific BK receptor antagonists. Pretreatment of cells with the B2 BK receptor antagonist HOE140 (1~100 nM) inhibited the BK-induced COX-2 expression in a concentration-dependent manner, while the B1 BK receptor antagonist (Lys-(Leu^8)des-Arg^9-BK) (10 and 100 μM) had no effect. When cells were treated with 100 nM HOE140, BK-induced COX-2 expression was inhibited by 58 ± 28% (n = 3) (Fig. 1*C*). Therefore, BK-stimulated COX-2 expression in A549 cells is mediated primarily through B2 BK receptors.

Augmentation of COX-2 expression occurred at the level of transcription

A549 cells were pretreated with either actinomycin D (a transcriptional inhibitor) or cycloheximide (a translational inhibitor) and then treated with 10 nM BK. As a result, the BK-induced elevation of COX-2 expression was inhibited by actinomycin D (1 μM) and cycloheximide (3 μM) by ~91 ± 15% and 72 ± 19%, respectively (Fig. 2*A*). The results suggest that the increase in COX-2 protein in A549 cells responsive to BK may have been due to COX-2 transcriptional expression.

NF-κB is involved in BK-induced COX-2 expression

As previously mentioned, NF-κB activation is necessary for COX-2 induction. Pyrrolidine dithiocarbate (PDTC), an antioxidant, has been shown to inactivate NF-κB in macrophages (30). To examine whether NF-κB activation is involved in the signal transduction pathway leading to COX-2 expression caused by BK, the NF-κB inhibitor, PDTC, was used. Fig. 2*B* shows that BK-induced increase in COX-2 protein levels was inhibited by PDTC (3 and 10 μM). When cells were treated with 10 μM PDTC, BK-induced COX-2 expression was inhibited by 87 ± 10% (n = 3). In parallel with the inhibition by PDTC, an IκB protease inhibitor (L-1-tosylamido-2-phenylenylethyl chloromethyl ketone (TPCK), 3 and 10 μM) (31) also inhibited BK-induced COX-2 protein expression. Pretreatment of cells with 10 μM TPCK completely abolished the BK response (Fig. 2*B*). To further confirm the role of NF-κB in the regulation of COX-2 expression, the human COX-2 promoter (−327/+59) or the κB site (−223/−214) deletion mutant (κBM) luciferase plasmid was transfected into A549 cells. As shown in Fig. 2*C*, 10 nM BK induced a 2.1-fold increase in COX-2 luciferase activity in cells transfected with the human COX-2 construct.

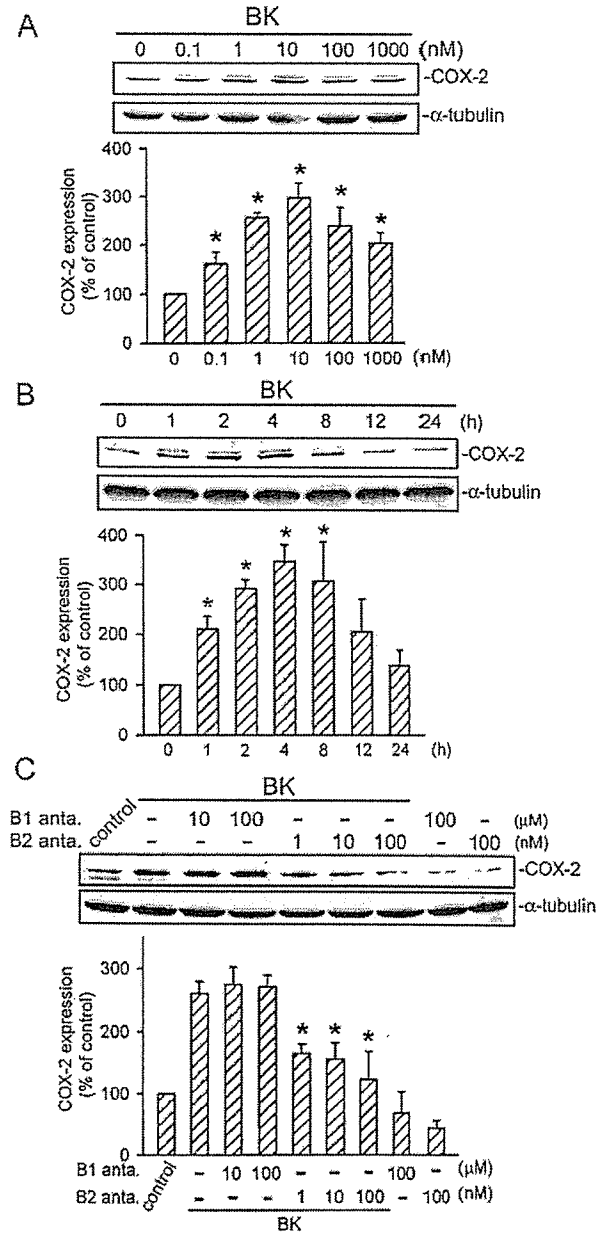

FIGURE 1. BK-induced COX-2 expression is mediated through B2 but not B1 BK receptors in A549 cells. Cells were incubated with various concentrations of BK for 4 h (*A*) or 10 nM BK for the indicated time intervals (*B*), and then COX-2 or α-tubulin protein levels were determined. Equal loading in each lane is shown by the similar intensities of α-tubulin. Traces represent results from three independent experiments, which are presented as the mean ± SE. *, $p < 0.05$ as compared with the control group. *C*, Cells were pretreated with the B1 BK receptor antagonist (B1 anta.), Lys-(Leu^8)des-Arg^9-BK (10~100 μM), or the B2 BK receptor antagonist (B2 anta.), HOE140 (1~100 nM), for 30 min, and then stimulated with 10 nM for 4 h. Cell were lysed, and then immunoblotted for COX-2 or α-tubulin. Equal loading in each lane is demonstrated by the similar intensities of α-tubulin. Traces represent results from three independent experiments, which are presented as the mean ± SE. *, $p < 0.05$ as compared with BK treatment.

BK-induced COX-2 luciferase activity was reduced by 67 ± 6% (n = 4) in cells transfected with the κBM construct. The results indicate that NF-κB activation is necessary for BK-induced COX-2 expression in A549 cells.

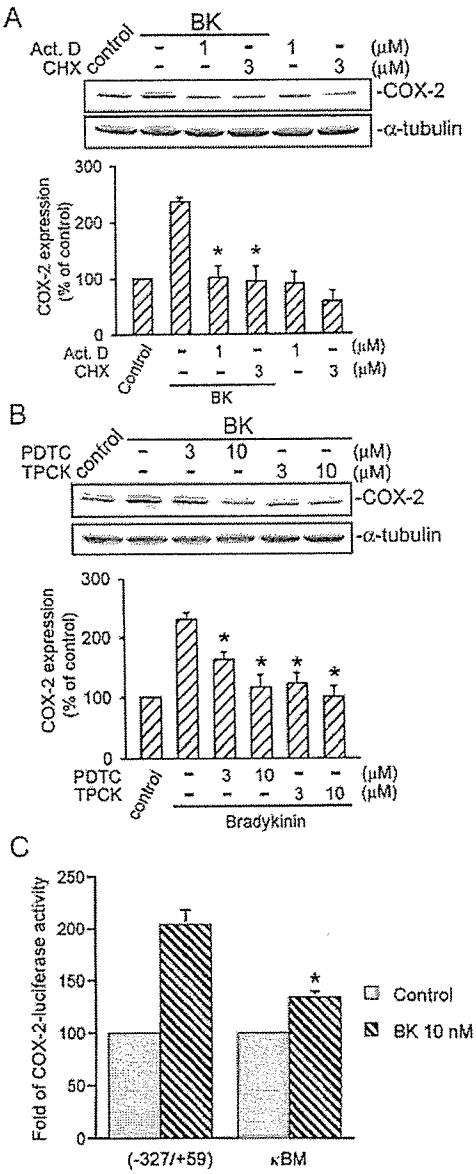

FIGURE 2. NF-κB is involved in BK-mediated COX-2 expression in A549 cells. *A*, BK-induced COX-2 expression involved transcriptional activity. Cells were pretreated for 30 min with 1 μM actinomycin D (Act. D) or 3 μM cycloheximide (CHX), and then stimulated with 10 nM BK for 4 h. Cells were lysed, and then immunoblotted for COX-2 or α-tubulin. *B*, The NF-κB signal pathway was necessary for BK-induced COX-2 expression. Cells were pretreated with various concentrations of PDTC or TPCK for 30 min, and then stimulated with 10 nM BK for 4 h. Cells were lysed, and then immunoblotted for COX-2 or α-tubulin. Equal loading in each lane is demonstrated by the similar intensities of α-tubulin. Traces represent results from three independent experiments, which are presented as the mean ± SE. *, $p < 0.05$ as compared with BK treatment. *C*, Cells were transfected with the COX-2 promoter (−327/+59) or the κB site (−223/−214) deletion mutant (κBM) luciferase expression vector, and then treated with 10 nM BK for 24 h. Luciferase activities were determined as described in *Materials and Methods*. The level of induction of luciferase activity was compared with that of cells without BK treatment. Data represent the mean ± SE. *, $p < 0.05$ as compared with BK on cells transfected with the COX-2 promoter (−327/+57).

BK induces NF-κB activation

NF-κB activation was directly evaluated by the translocation of NF-κB from the cytosol to the nucleus and a gel shift DNA-binding assay. Treatment of cells with 10 nM BK resulted in marked

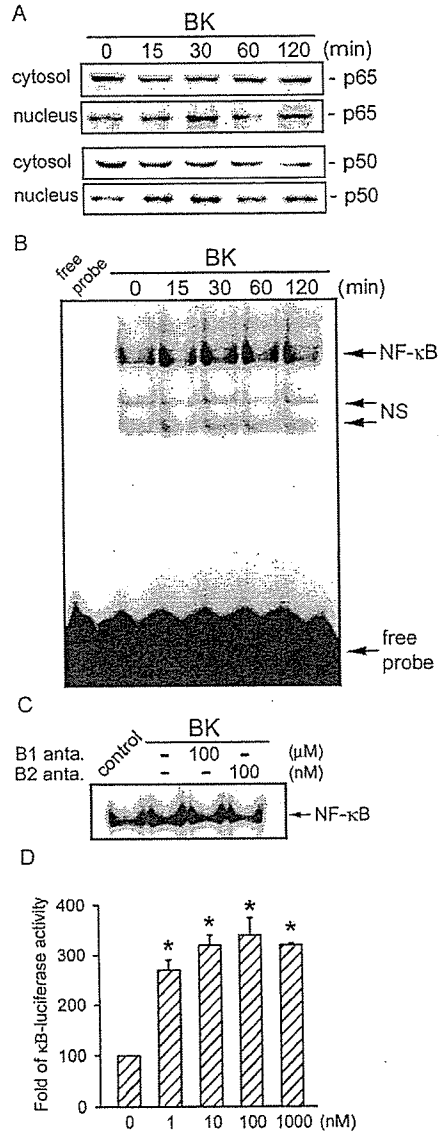

FIGURE 3. BK induced increases in p65 and p50 translocation, NF-κB-specific DNA-protein complex formation, and κB-luciferase activity in A549 cells. *A*, Time-dependent translocation of p65 and p50 by BK. Cells were treated with 10 nM BK for 0~120 min, and then cytosol and nucleus fractions were prepared as described in *Materials and Methods*. Levels of cytosolic and nuclear p65 and p50 were determined by immunoblotting with p65- and p50-specific Abs, respectively. Typical traces are representative of three experiments with similar results. *B*, Time-dependent activation of NF-κB by BK. A549 cells were incubated with 10 nM BK for 0~120 min. Following incubation, a nuclear extract was prepared, and EMSA was performed as described in *Materials and Methods*. The top band represents NF-κB. NS, Nonspecific binding. *C*, BK-mediated NF-κB activation is mediated by the B2 BK receptor. A549 cells were pretreated with the B1 BK receptor antagonist (B1 anta.), Lys-(Leu^8)des-Arg^9-BK (100 μM), or the B2 BK receptor antagonist (B2 anta.), HOE140 (100 nM), for 30 min followed by stimulation with 10 nM BK for another 30 min. Nuclear extracts were prepared for determination of NF-κB-specific DNA protein-binding activity by EMSA. *D*, Concentration-dependent-induced κB-luciferase activity by BK. Cells were transiently transfected with 0.5 μg of pGL2-ELAM-Luc and 1 μg of pBK-CMV-Lac Z for 24 h, and then cells were incubated with 1~1000 nM BK for another 24 h. Luciferase activities were determined as described in *Materials and Methods*. The level of induction of luciferase activity was compared with that of cells without BK treatment. Data represent the mean ± SE of three experiments performed in duplicate. *, $p < 0.05$ as compared with the control without BK treatment.

translocation of p65 and p50 NF-κB from the cytosol to the nucleus which began at 15 min, peaked at 30 min, and then had declined after 60 min of treatment (Fig. 3*A*). In nuclear extracts of unstimulated cells, a slight intensity of NF-κB-specific DNA-protein complex formation was observed. Stimulation of cells with 10 nM BK resulted in time-dependent activation of NF-κB-specific DNA-protein complex formation, with a maximum effect after 30 min of treatment. However, after 60 min of treatment with BK, the intensities of these DNA-protein complexes had decreased (Fig. 3*B*). Pretreatment of cells for 30 min with the B2 BK receptor antagonist HOE140 (100 nM) markedly attenuated BK-induced formation of NF-κB-specific DNA-protein complexes, while the B1 BK receptor antagonist, (Lys-(Leu^8)des-Arg^9-BK) (100 μM), had no effect (Fig. 3*C*). Therefore, BK-stimulated NF-κB activation in A549 cells is mediated primarily through the B2 BK receptor. To directly determine NF-κB activation after BK treatment, A549 cells were transiently transfected with pGL2-ELAM-κB-luciferase as an indicator of NF-κB activation. As shown in Fig. 3*D*, cells treated with BK (1~1000 nM) for 24 h caused a concentration-dependent increase in κB-luciferase activity with about a 230 ± 18% (n = 3) increase after 10 nM BK treatment.

BK causes increases in IKKαβ phosphorylation, IKKαβ activity, IκBα phosphorylation, and IκBα degradation

We further determined the upstream molecules of NF-κB in BK-induced NF-κB activation. Stimulation of cells with 10 nM BK induced an increase in IKKαβ phosphorylation and IKKαβ activity in time-dependent manners, reaching a maximum after 5 and 10 min of treatment, respectively (Fig. 4*A* and *B*). In parallel with IKKαβ phosphorylation and IKKαβ activity, IκBα phosphorylation was apparent after 10 min of treatment with 10 nM BK, and it reached a maximum effect after 20 min of treatment (Fig. 4*C*). Furthermore, it also caused IκBα degradation after 20 min of treatment with 10 nM BK, and the IκBα protein had been resynthesized after 60 min of treatment (Fig. 4*D*).

Ras is involved in BK-induced COX-2 expression

To explore whether Ras might mediate BK-induced COX-2 expression, manumycin A, a Ras inhibitor (32) was used. As shown in Fig. 5*A*, pretreatment of A549 cells with manumycin A (0.3~3 μM) inhibited BK-induced COX-2 expression in a concentration-dependent manner. When cells were treated with 3 μM manumycin A, BK-induced COX-2 expression was inhibited by 63 ± 11% (n = 3) (Fig. 5*A*). Next, we directly measured the Ras activity in response to BK. Fig. 5*B* shows that treatment of A549 cells with 10 nM BK induced an increase in Ras activity in a time-dependent manner, as assessed by immunoblotting samples for Ras immunoprecipitated from lysates using Raf-1 RBD. Maximal activation was detected after 5~10 min of stimulation, and the response continued until 30 min of stimulation (Fig. 5*B*). The BK-induced increase in Ras activity was markedly inhibited by pretreatment of cells for 30 min with manumycin A (1 and 3 μM) in a concentration-dependent manner (Fig. 5*C*). Taken together, these results imply that Ras activation is involved in BK-induced COX-2 expression.

Raf-1 is involved in BK-induced COX-2 expression

To examine whether Raf-1, a target protein for Ras, might play a crucial role in BK-induced COX-2 expression, the Raf-1 inhibitor,

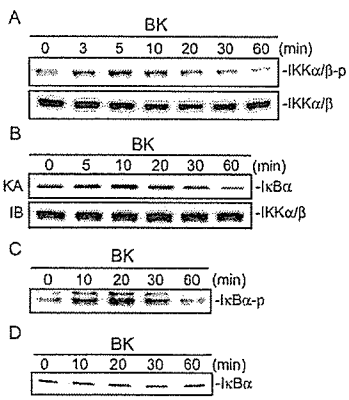

FIGURE 4. BK induced increases in IKKαβ phosphorylation, IKKαβ activity, IκBα phosphorylation, and IκBα degradation in A549 cells. *A*, Cells were incubated with 10 nM BK for the indicated time intervals. Whole cell lysates were prepared, and then immunoblotted with Abs for phospho-IKKαβ or -IKKαβ, respectively. *B*, A549 cells were incubated with 10 nM BK for 0~60 min, and then cell lysates were immunoprecipitated with Abs specific for IKKα and IKKβ. One set of immunoprecipitates was subjected to the kinase assay (KA) using the GST-IκBα fusion protein as a substrate (*top panel*). The other set of immunoprecipitates was subjected to 10% SDS-PAGE and analyzed by immunoblotting (IB) with anti-IKKαβ Ab (*bottom panel*). Equal amounts of the immunoprecipitated kinase complex present in each kinase assay were confirmed by immunoblotting for IKKαβ. *C* and *D*, Following incubation for 0~120 min with 10 nM BK, IκBα phosphorylation (*C*) and IκBα degradation (*D*) were determined by immunoblotting using phospho-IκBα- and IκBα-specific Abs, respectively. Typical traces are representative of three experiments with similar results.

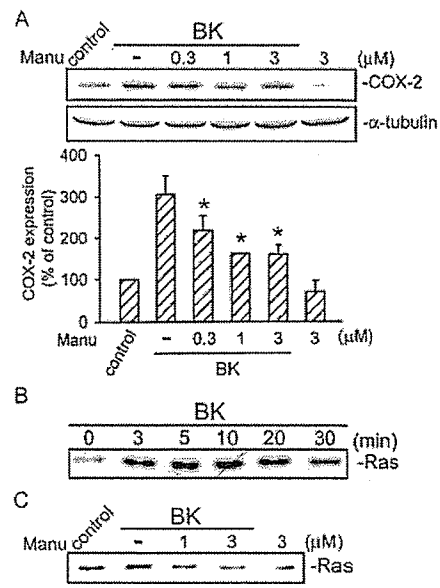

FIGURE 5. Effects of manumycin A on BK-induced COX-2 expression and Ras activation in A549 cells. *A*, Cells were pretreated with vehicle and manumycin A (0.3~3 μM) for 30 min, followed by stimulation with 10 nM BK for another 4 h, and COX-2 expression was determined by immunoblotting with an Ab specific for COX-2. Equal loading in each lane is demonstrated by the similar intensities of α-tubulin. Typical traces are representative of two experiments with similar results, which are presented as the mean ± SE. *, $p < 0.05$ as compared with BK treatment. *B*, A549 cells were incubated with 10 nM BK for 0~30 min, and then cell lysates were immunoprecipitated with an Ab specific for Raf-1 RBD. The Ras activity assay is described in *Materials and Methods*. Typical traces represent two experiments with similar results. *C*, Cells were pretreated with manumycin A (1 and 3 μM) for 30 min, and then treated with 10 nM BK for another 5 min. Cells were then lysed for the Ras activity assay as described above. Typical traces represent two experiments with similar results.

GW 5074 (33), was used. As shown in Fig. 6*A*, pretreatment of A549 cells with GW 5074 (0.3~3 nM) concentration-dependently inhibited BK-induced COX-2 expression. Treatment of cells with 3 nM GW 5074 slightly affected the basal COX-2 level, but it almost completely inhibited BK-induced COX-2 expression. Raf-1 is associated with Ras-GTP, and then by additional modifications such as phosphorylation at Ser^{338}, becomes the active form (25). The activated Raf-1 then triggers sequential activation of downstream molecules. Thus, phosphorylation of Raf-1 at Ser^{338} is a critical step in Raf-1 activation. Next, we further examined Raf-1 Ser^{338} phosphorylation by BK stimulation in A549 cells using the anti-phospho-Raf-1 Ab at Ser^{338}. When cells were treated with 10 nM BK for various time intervals, Raf-1 Ser^{338} phosphorylation increased at 3 min and peaked at 5~10 min. After 30 min of treatment, the BK-induced Raf-1 Ser^{338} phosphorylation had declined (Fig. 6*B*). In addition, BK-induced Raf-1 Ser^{338} phosphorylation was inhibited by treatment with 1 μM manumycin A and 1 nM GW 5074 (Fig. 6*C*). The results indicate that Raf-1 is a downstream molecule of Ras and is involved in BK-mediated COX-2 protein expression.

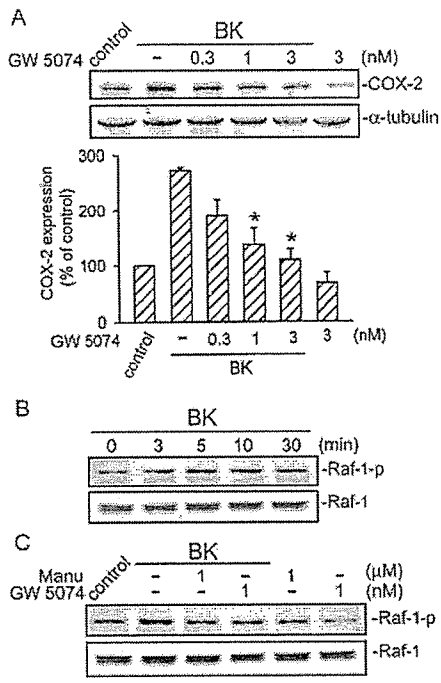

FIGURE 6. Effects of GW 5074 on BK-induced COX-2 expression and Raf-1 phosphorylation in A549 cells. *A*, Cells were pretreated with vehicle and GW 5074 (0.3~3 nM) for 30 min, followed by stimulation with 10 nM BK for another 4 h, and COX-2 expression was determined by immunoblotting with a specific COX-2 Ab. Equal loading in each lane is demonstrated by the similar intensities of α-tubulin. Typical traces represent three experiments with similar results, which are presented as the mean ± SE. *, $p < 0.05$ as compared with BK treatment. *B*, A549 cells were incubated with 10 nM BK for 0~30 min, and then Raf-1 phosphorylation (*upper panel*) and Raf-1 (*bottom panel*) protein levels were determined. The presence of equal loading in each lane is shown by the similar intensities of Raf-1. Traces represent results from three independent experiments. *C*, Cells were pretreated with manumycin A (1 μM) or GW 5074 (1 nM) for 30 min, and then treated with 10 nM BK for another 5 min. Cells were then lysed for Raf-1 phosphorylation (*upper panel*) and Raf-1 (*bottom panel*) protein levels as described above. Typical traces represent two experiments with similar results.

ERK is involved in BK-induced COX-2 expression

We next wished to determine whether BK is able to activate ERK, a critical downstream target of Raf-1 (34), which has been shown to induce gene expression (35). We tested the role of ERK in BK-induced COX-2 expression by using the specific MEK inhibitor, PD 098059. As shown in Fig. 7*A*, BK-induced COX-2 expression was markedly attenuated by pretreatment of cells with PD 098059 (3~30 μM) in a concentration-dependent manner. Pretreatment of cells with 30 μM PD 098059 inhibited BK-induced COX-2 expression by 77 ± 14% ($n = 3$). To directly confirm the crucial role of ERK in COX-2 expression, we determined ERK

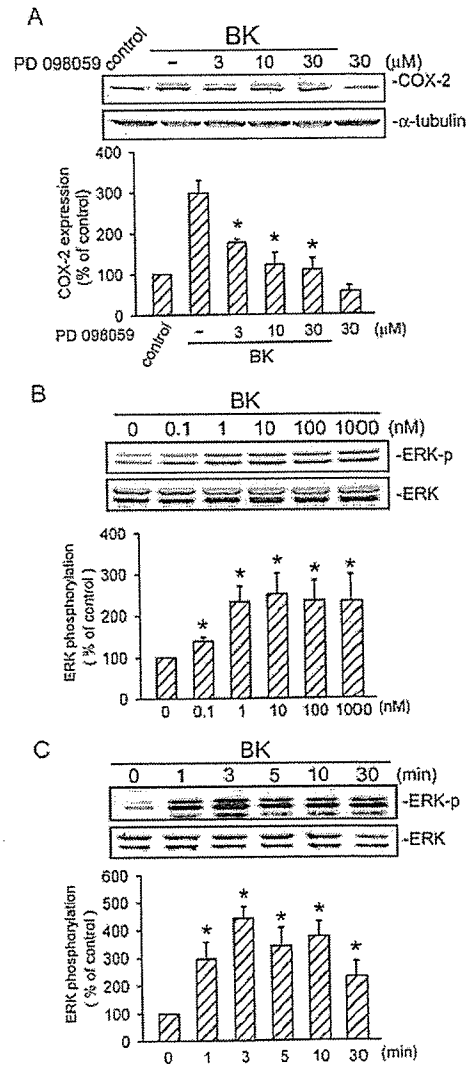

FIGURE 7. ERK is involved in BK-mediated COX-2 expression in A549 cells. *A*, Cells were pretreated with vehicle and PD 098059 (3~30 μM) for 30 min before treatment with 10 nM BK for another 4 h, and COX-2 expression was determined by immunoblotting with a specific COX-2 Ab. Equal loading in each lane is shown by the similar intensities of α-tubulin. Typical traces represent three experiments with similar results, which are presented as the mean ± SE. *, $p < 0.05$ as compared with BK treatment. *B* and *C*, Cells were treated with various concentrations of BK for 3 min (*B*) or 10 nM BK for different time intervals (*C*). ERK phosphorylation was shown by immunoblotting with an Ab specific for phosphorylated ERK (p-ERK) (*upper panel*). Equal loading in each lane is shown by the similar intensities of ERK2 (*bottom panel*). Traces represent results from three independent experiments, which are presented as the mean ± SE. *, $p < 0.05$ as compared with the control group.

phosphorylation in response to BK. As shown in Fig. 7*B*, treatment with BK (0.1~1000 nM) for 3 min induced ERK phosphorylation in a concentration-dependent manner, with a maximum effect at 10 nM BK treatment. Stimulation of cells with 10 nM BK resulted in time-dependent phosphorylation of ERK. ERK phosphorylation began at 1 min, peaked at 3 min, and then had declined after 5 min of BK treatment (Fig. 7*C*). The protein level of ERK2 was not affected by BK treatment (Fig. 7, *B* and *C*, *bottom panel*). Pretreatment of cells with HOE140 (1~100 nM) inhibited BK-induced ERK activation in a concentration-dependent manner, while (Lys-(Leu^8)des-Arg^9-BK) (10 and 100 μM) had no effect (Fig. 8*A*). None of these treatments had any effect on ERK expression (Fig. 8*A*, *bottom panel*). Therefore, BK-stimulated ERK activation is mediated through the B2 BK receptor. We further examined the relationships among Ras, Raf-1, MEK, and ERK in the BK-mediated signaling pathway. When cells were pretreated for 30 min with PD 098059 (3~30 μM) or the p38 MAPK inhibitor, SB 203580 (0.01~1 μM), BK-induced ERK activation was markedly inhibited by PD 098059 in a concentration-dependent manner, but not by SB 203580 at concentrations of up to 1 μM (Fig. 8*B*). Pretreatment of A549 cells for 30 min with 3 μM manumycin A or 3 nM GW 5074 markedly inhibited BK-induced ERK phosphorylation (Fig. 8*B*). None of these treatments had any effect on ERK expression (Fig. 8 *B* and *C*, *bottom panel*). Based on these results, we suggest that activations of Ras, Raf-1, and MEK occur upstream of ERK in the BK-induced signaling pathway.

Ras, Raf-1, and ERK mediate BK-induced IKK$\alpha\beta$ and NF-κB activation

We further examined whether activation of IKK$\alpha\beta$ and NF-κB occurs through the Ras/Raf-1/ERK signaling pathway. As shown in Fig. 9*A*, pretreatment of cells for 30 min with 3 μM manumycin A, 3 nM GW 5074, and 30 μM PD 098059 markedly attenuated the BK-induced increase in IKK$\alpha\beta$ activity. To further confirm the role of Ras in BK-mediated IKK$\alpha\beta$ activation, a Ras dominant-negative mutant (RasN17) was tested. Transfection of A549 cells with 1 μg of RasN17 inhibited the BK-induced increase in IKK$\alpha\beta$ activity (Fig. 9*A*). Similarly, when cells were pretreated for 30 min with 3 μM manumycin A, 3 nM GW 5074, and 30 μM PD 098059, BK-induced formation of NF-κB-specific DNA-protein complexes was markedly inhibited by manumycin A, GW 5074, and PD 098059 (Fig. 9*B*). Moreover, transfection of A549 cells with 1 μg RasN17 also inhibited the BK-induced effects (Fig. 9*B*). Taken together, these data suggest that activation of the Ras/Raf-1/ERK pathway is also required for BK-induced IKK$\alpha\beta$ and NF-κB activation in A549 cells.

Discussion

BK is recognized to play an important role in asthma. Several studies have shown that BK is generated in human airways within minutes of an allergen challenge (36). Allergen challenge studies have also established that BK plays a pivotal role in the initiation of chronic airway inflammation (37). B2 BK receptor antagonists effectively block the development of the late-phase airway response as well as the development of bronchial hyperresponsiveness following allergen challenge in a number of different experimental animal models (3, 4). To explore the mechanism by which BK promotes airway inflammation, we examined the ability of BK to regulate COX-2 expression in airway epithelial cells. We found that BK can induce COX-2 expression in airway epithelial cells. Similar results were also seen in human airway smooth muscle cells and fibroblasts (14, 15). Because asthmatic patients have elevated levels of kinin concentrations in nasal fluid and bronchoalveolar fluid (38, 39),

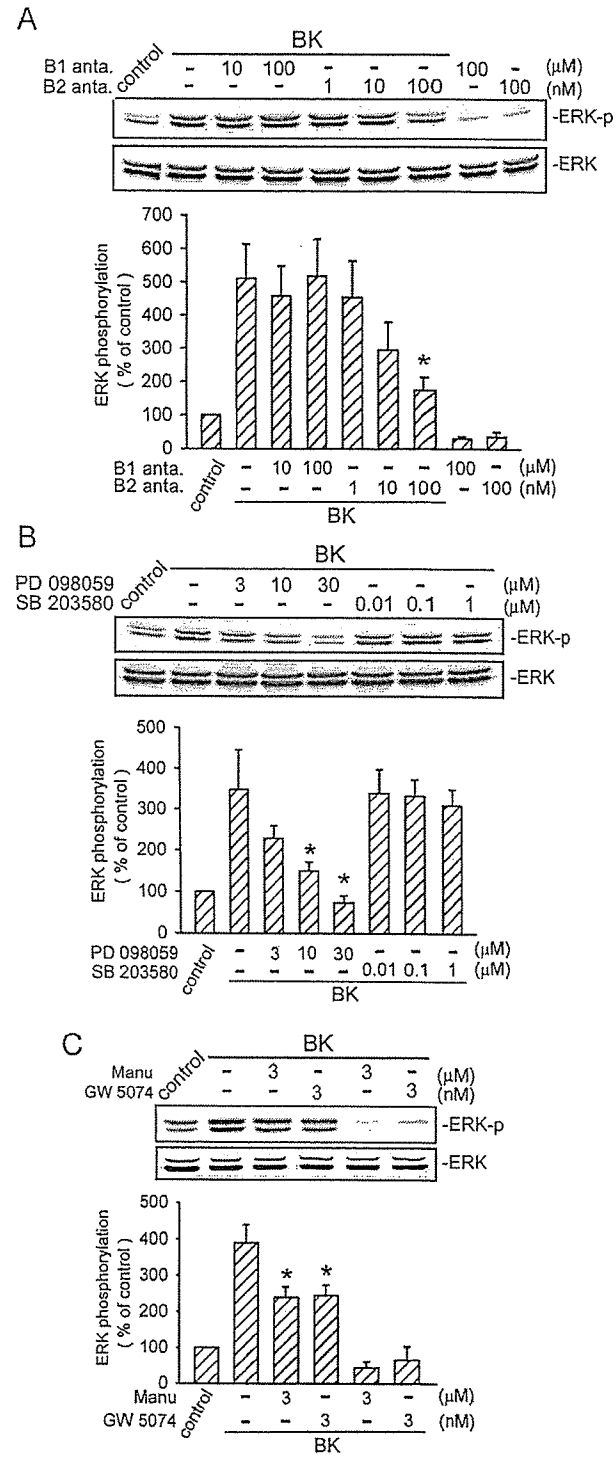

FIGURE 8. Mediation of BK-induced ERK activation through B2 BK receptors and involvement of the Ras/Raf-1/MEK signal pathway in BK-mediated ERK activation in A549 cells. *A*, Cells were pretreated with the B1 BK receptor antagonist (B1 anta.), Lys-(Leu^8)des-Arg^9-BK (10~100 μM), or the B2 BK receptor antagonist (B2 anta.), HOE140 (1~100 nM), for 30 min, and then stimulated with 10 nM BK for 3 min. *B* and *C*, Cells were pretreated with various concentrations of PD 098059 or SB 203580 (*B*), manumycin A or GW 5074 (*C*) for 30 min, and then incubated with 10 nM BK for another 3 min. Whole cell lysates were prepared and subjected to immunoblotting analysis using Abs specific for phosphorylated ERK (ERK-p) (*upper panel*) or nonphosphorylated ERK (ERK) (*bottom panel*). The extent of ERK activation was quantified using a densitometer with Image-Pro plus software Media Cybernetics (Silver Spring, MD). Traces represent results from three independent experiments, which are presented as the mean ± SE. *, $p < 0.05$ as compared with BK treatment.